J|A|C|S ARTICLES

Published on Web 12/03/2009

Dearomatization Reactions of N-Heterocycles Mediated by Group 3 Complexes

Kevin L. Miller,[†] Bryan N. Williams,[†] Diego Benitez,[‡] Colin T. Carver,[†] Kevin R. Ogilby,[†] Ekaterina Tkatchouk,[‡] William A. Goddard III,[‡] and Paula L. Diaconescu*,[†]

Department of Chemistry & Biochemistry, University of California, Los Angeles, California 90095, and Materials and Process Simulation Center, California Institute of Technology, Pasadena, California 91125

Received October 13, 2009; E-mail: pld@chem.ucla.edu

Abstract: Group 3 (Sc, Y, Lu, La) benzyl complexes supported by a ferrocene diamide ligand are reactive toward aromatic N-heterocycles by mediating their coupling and, in a few cases, the cleavage of their C−N bonds. When these complexes reacted with 2,2′-bipyridine or isoquinoline, they facilitated the alkyl migration of the benzyl ligand onto the pyridine ring, a process accompanied by the dearomatization of the N-heterocycle. The products of the alkyl-transfer reactions act as hydrogen donors in the presence of aromatic N-heterocycles, ketones, and azobenzene. Experimental and computational studies suggest that the hydrogen transfer takes place through a concerted mechanism. An interesting disproportionation reaction of the dearomatized, alkyl-substituted isoquinoline complexes is also reported.

Introduction

Early transition metal alkyl or hydride complexes often react with aromatic N-heterocycles to produce ortho-metalated complexes.[1−19] Such ortho-metalation reactions take place through a σ-bond metathesis mechanism,[16,20−22] in which the alkyl group on the metal engages the hydrogen atom on the α-carbon of the heterocyclic ring and is eliminated as the corresponding hydrocarbon. Less commonly, alkyl ligands of early transition metal complexes will undergo a 1,3-alkyl migration, when they are transferred to the α-carbon of the coordinated N-heterocycle.[23−25] Alkyl migration may occur occasionally to other positions of the heteroaromatic ring.[19] In some instances, the alkyl migration[26] is followed by the C−N bond cleavage of the aromatic heterocycle,[27−29] a reaction relevant to the study of hydrodenitrogenation processes.[30−35]

[†] University of California, Los Angeles.
[‡] California Institute of Technology.

(1) Diaconescu, P. L. *Curr. Org. Chem.* **2008**, *12*, 1388–1405.
(2) Boaretto, R.; Roussel, P.; Kingsley, A. J.; Munslow, I. J.; Sanders, C. J.; Alcock, N. W.; Scott, P. *Chem. Commun.* **1999**, 1701–1702.
(3) Boaretto, R.; Roussel, P.; Alcock, N. W.; Kingsley, A. J.; Munslow, I. J.; Sanders, C. J.; Scott, P. *J. Organomet. Chem.* **1999**, *591*, 174–184.
(4) den Haan, K. H.; Wielstra, Y.; Teuben, J. H. *Organometallics* **1987**, *6*, 2053–2060.
(5) Dormond, A.; El Bouadili, A. A.; Moïse, C. *J. Chem. Soc., Chem. Commun.* **1985**, 914–916.
(6) Duchateau, R.; Brussee, E. A. C.; Meetsma, A.; Teuben, J. H. *Organometallics* **1997**, *16*, 5506–5516.
(7) Duchateau, R.; van Wee, C. T.; Teuben, J. H. *Organometallics* **1996**, *15*, 2291–2302.
(8) Jantunen, K. C.; Scott, B. L.; Kiplinger, J. L. *J. Alloys Compd.* **2007**, *444*−*445*, 363–368.
(9) Jordan, R. F.; Guram, A. S. *Organometallics* **1990**, *9*, 2116–2123.
(10) Kiplinger, J. L.; Scott, B. L.; Schelter, E. J.; Pool Davis Tournear, J. A. *J. Alloys Compd.* **2007**, *444*−*445*, 477–482.
(11) Klei, B.; Teuben, J. H. *J. Chem. Soc., Chem. Commun.* **1978**, 659–660.
(12) Klei, E.; Teuben, J. H. *J. Organomet. Chem.* **1981**, *214*, 53–64.
(13) Pool, J. A.; Scott, B. L.; Kiplinger, J. L. *J. Alloys Compd.* **2006**, *418*, 178–183.
(14) Radu, N. S.; Buchwald, S. L.; Scott, B.; Burns, C. J. *Organometallics* **1996**, *15*, 3913–3915.
(15) Scollard, J. D.; McConville, D. H.; Vittal, J. J. *Organometallics* **1997**, *16*, 4415–4420.
(16) Thompson, M. E.; Baxter, S. M.; Bulls, A. R.; Burger, B. J.; Nolan, M. C.; Santarsiero, B. D.; Schaefer, W. P.; Bercaw, J. E. *J. Am. Chem. Soc.* **1987**, *109*, 203–219.
(17) Watson, P. L. *J. Chem. Soc., Chem. Commun.* **1983**, 276–277.
(18) Jantunen, K. C.; Scott, B. L.; Gordon, J. C.; Kiplinger, J. L. *Organometallics* **2007**, *26*, 2777–2781.
(19) Sugiyama, H.; Aharonian, G.; Gambarotta, S.; Yap, G. P. A.; Budzelaar, P. H. M. *J. Am. Chem. Soc.* **2002**, *124*, 12268–12274.
(20) Bercaw, J. E. *Pure Appl. Chem.* **1990**, *62*, 1151–1154.
(21) Watson, P. L. *J. Am. Chem. Soc.* **1983**, *105*, 6491–6493.
(22) Watson, P. L.; Parshall, G. W. *Acc. Chem. Res.* **1985**, *18*, 51–56.
(23) Jantunen, K. C.; Scott, B. L.; Hay, P. J.; Gordon, J. C.; Kiplinger, J. L. *J. Am. Chem. Soc.* **2006**, *128*, 6322–6323.
(24) Cameron, T. M.; Gordon, J. C.; Scott, B. L.; Tumas, W. *Chem. Commun.* **2004**, 1398–1399.
(25) Reardon, D.; Conan, F.; Gambarotta, S.; Yap, G.; Wang, Q. *J. Am. Chem. Soc.* **1999**, *121*, 9318–9325.
(26) Scott, J.; Gambarotta, S.; Korobkov, I.; Budzelaar, P. H. M. *J. Am. Chem. Soc.* **2005**, *127*, 13019–13029.
(27) Pool, J. A.; Scott, B. L.; Kiplinger, J. L. *Chem. Commun.* **2005**, 2591–2593.
(28) Gray, S. D.; Weller, K. J.; Bruck, M. A.; Briggs, P. M.; Wigley, D. E. *J. Am. Chem. Soc.* **1995**, *117*, 10678–10693.
(29) Weller, K. J.; Gray, S. D.; Briggs, P. M.; Wigley, D. E. *Organometallics* **1995**, *14*, 5588–5597.
(30) Katzer, J. R.; Sivasubramanian, R. *Catal. Rev.-Sci. Eng.* **1979**, *20*, 155–208.
(31) Ho, T. C. *Catal. Rev.-Sci. Eng.* **1988**, *30*, 117–160.
(32) Perot, G. *Catal. Today* **1991**, *10*, 447–472.
(33) Prins, R. In *A Handbook of Heterogeneous Catalysis*; Ertl, G., Knözinger, H., Weitkamp, J., Eds.; VCH Verlagsgesellschaft: Weinheim, Germany, 1997.
(34) Kabe, T.; Ishikawa, A.; Qian, W. *Hydrodesulfurization and Hydrodenitrogenation*; Wiley-VCH: Chichester, UK, 1999.

10.1021/ja908489p

The cleavage of aromatic C−N bonds is relatively rare[27,36−52] and the dearomatization of N-heterocycles may be the first step in developing a methodology for their C−N bond cleavage.[1,42,53]

Our group has previously reported several reactions mediated by the scandium, yttrium, and lutetium alkyl complexes $(NN^{fc})M(CH_2Ar)(THF)$, **1^{M}−THF** (NN^{fc} = fc(NSi^{t}BuMe$_2$)$_2$, fc = 1,1′-ferrocenylene; M = Sc, Lu: Ar = 3,5-Me$_2$C$_6$H$_3$; M = Y: Ar = C$_6$H$_5$), in which pyridines have been C−H activated at the α-carbon (Scheme 1).[51,54,55] These ortho-metalated complexes were supported by the silylated ferrocene diamide ligand NN^{fc} [51,54−58] and underwent subsequent coupling and isomerization reactions (Scheme 1).[51,55] The isomerization reaction entailed the migration of a hydrogen atom within a single heterocyclic ring. On the basis of DFT computational studies, we proposed that the mechanism involved a transition state in which the heterocyclic ring adopted a boat-like conformation, allowing the hydrogen to migrate between the two carbon atoms involved in the process.

In addition to the C−H activation of aromatic N-heterocycles, we have found that an alkyl migration takes place when substrates such as isoquinoline and 2,2′-bipyridine are employed in reactions with group 3 (scandium, yttrium, lutetium, and lanthanum) benzyl complexes. Herein we report the synthesis and characterization of these products and their subsequent reactivity with unsaturated substrates. These reactions also involve hydrogen transfer; however, in contrast to the previous isomerization process, the hydrogen is transferred between two separate rings and the mechanism involves metalocycles as intermediates. DFT computational studies were undertaken to provide insight and support the proposed mechanism. The present report represents the first combined experimental and computational systematic study of alkyl migration to aromatic N-heterocycles involving group 3 complexes and of the subsequent reactions of these products. These results complement those reported for transition-metal olefin polymerization catalysts supported by derivatized aromatic N-heterocyclic ligands.[25,26,59,60]

Scheme 1. Reactions of 2-Phenylpyridine Mediated by the Alkyl Complexes **1^{M}−THF** (M = Sc/Y/Lu)

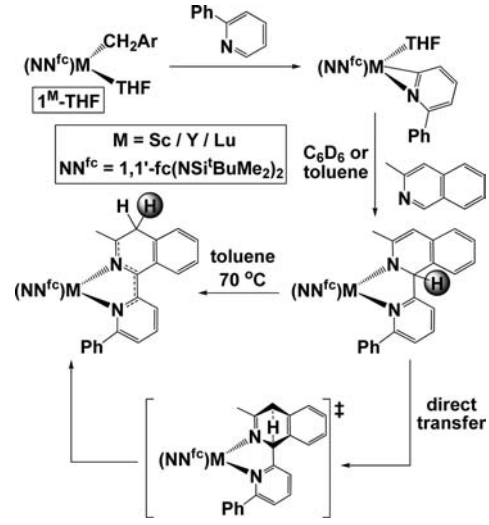

Results and Discussion

Synthesis and Characterization of Complexes. The complexes **1^{M}−THF** had been previously characterized for scandium, yttrium, and lutetium.[51,55,56] In the present work, this chemistry is extended to lanthanum, $(NN^{fc})La(CH_2Ph)(THF)$ (**1^{La}−THF**), which allows a comparison of the reactivity behavior of the group 3 benzyl complexes across a wider range of atomic radii than before. In addition, the complex $La(CH_2Ar)_3(THF)_3$ (Ar = 3,5-Me$_2$C$_6$H$_3$) was prepared and characterized as a precursor to **1′^{La}−THF** (Ar = 3,5-Me$_2$C$_6$H$_3$). The 3,5-Me$_2$C$_6$H$_3$ group was chosen initially because it improved the solubility of the corresponding scandium and lutetium complexes; however, $La(CH_2Ar)_3(THF)_3$ (Ar = 3,5-Me$_2$C$_6$H$_3$) was more difficult to prepare and store than its scandium and lutetium counterparts. Therefore, most reactivity studies presented in this work were carried out with **1^{La}−THF** (Ar = Ph), for which $La(CH_2Ph)_3(THF)_3$ was used as a precursor.

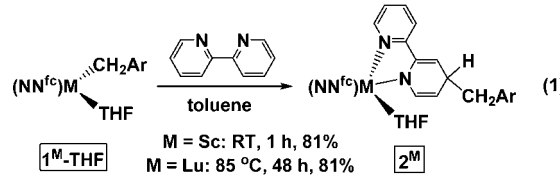

In order to test the scope of the aromatic N-heterocycle ortho-metalation reaction,[51,54,55] a biheterocyclic substrate, 2,2′-

(35) Furimsky, E.; Massoth, F. E. *Catal. Rev.-Sci. Eng.* **2005**, *47*, 297–489 and references therein.
(36) Gray, S. D.; Weller, K. J.; Bruck, M. A.; Briggs, P. M.; Wigley, D. E. *J. Am. Chem. Soc.* **1995**, *117*, 10678–10693.
(37) Gray, S. D.; Smith, D. P.; Bruck, M. A.; Wigley, D. E. *J. Am. Chem. Soc.* **1992**, *114*, 5462–5463.
(38) Weller, K. J.; Gray, S. D.; Briggs, P. M.; Wigley, D. E. *Organometallics* **1995**, *14*, 5588–5597.
(39) Weller, K. J.; Filippov, I.; Briggs, P. M.; Wigley, D. E. *Organometallics* **1998**, *17*, 322–329.
(40) Weller, K. J.; Filippov, I.; Briggs, P. M.; Wigley, D. E. *J. Organomet. Chem.* **1997**, *528*, 225–228.
(41) Allen, K. D.; Bruck, M. A.; Gray, S. D.; Kingsborough, R. P.; Smith, D. P.; Weller, K. J.; Wigley, D. E. *Polyhedron* **1995**, *14*, 3315–3333.
(42) Weller, K. J.; Fox, P. A.; Gray, S. D.; Wigley, D. E. *Polyhedron* **1997**, *16*, 3139–3163 and references therein.
(43) Kleckley, T. S.; Bennett, J. L.; Wolczanski, P. T.; Lobkovsky, E. B. *J. Am. Chem. Soc.* **1997**, *119*, 247–248.
(44) Bonanno, J. B.; Veige, A. S.; Wolczanski, P. T.; Lobkovsky, E. B. *Inorg. Chim. Acta* **2003**, *345*, 173–184.
(45) Covert, K. J.; Neithamer, D. R.; Zonnevylle, M. C.; LaPointe, R. E.; Schaller, C. P.; Wolczanski, P. T. *Inorg. Chem.* **1991**, *30*, 2494–2508.
(46) Neithamer, D. R.; Parkanyi, L.; Mitchell, J. F.; Wolczanski, P. T. *J. Am. Chem. Soc.* **1988**, *110*, 4421–4423.
(47) Fout, A. R.; Bailey, B. C.; Tomaszewski, J.; Mindiola, D. J. *J. Am. Chem. Soc.* **2007**, *129*, 12640–12641.
(48) Bailey, B. C.; Fan, H.; Huffman, J. C.; Baik, M. H.; Mindiola, D. J. *J. Am. Chem. Soc.* **2006**, *128*, 6798–6799.
(49) Huertos, M. A.; Perez, J.; Riera, L. *J. Am. Chem. Soc.* **2008**, *130*, 5662–5663.
(50) Huertos, M. A.; Peérez, J.; Riera, L.; Meneéndez-Velázquez, A. *J. Am. Chem. Soc.* **2008**, *130*, 13530–13531.
(51) Carver, C. T.; Diaconescu, P. L. *J. Am. Chem. Soc.* **2008**, *130*, 7558–7559.
(52) Monreal, M. J.; Khan, S.; Diaconescu, P. L. *Angew. Chem., Int. Ed.* **2009**, *48*, 8352–8355.
(53) Sanchez-Delgado, R. A. *Organometallic modelling of the hydrodesulfurization and hydrodenitrogenation reactions*; Kluwer Academic Publishers: Dordrecht, The Netherlands, 2002.
(54) Carver, C. T.; Diaconescu, P. L. *J. Alloys Compd.* **2009**, *488*, 518−523.
(55) Carver, C. T.; Benitez, D.; Miller, K. L.; Williams, B. N.; Tkatchouk, E.; Goddard, W. A.; Diaconescu, P. L. *J. Am. Chem. Soc.* **2009**, *131*, 10269–10278.
(56) Carver, C. T.; Monreal, M. J.; Diaconescu, P. L. *Organometallics* **2008**, *27*, 363–370.
(57) Monreal, M. J.; Diaconescu, P. L. *Organometallics* **2008**, *27*, 1702–1706.
(58) Monreal, M. J.; Carver, C. T.; Diaconescu, P. L. *Inorg. Chem.* **2007**, *46*, 7226–7228.

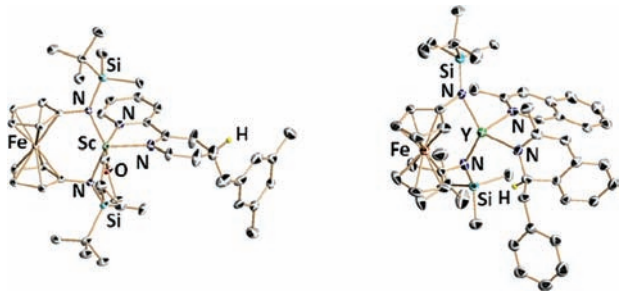

Figure 1. ORTEP representation of $\mathbf{2^{Sc}}$ (left) and $\mathbf{3^{Y}-iqn^{Me}}$ (right) with ellipsoids drawn at the 50% probability level (irrelevant hydrogen atoms were removed for clarity).

bipyridine, was mixed with the alkyl complexes $\mathbf{1^{M}-THF}$ (M = Sc, Lu). However, instead of the C−H activation reaction encountered with pyridines, the product of alkyl transfer was observed (eq 1, $\mathbf{2^{M}}$). The concomitant dearomatization of one of the pyridine rings was indicated in the ^{1}H NMR spectrum of the scandium product $\mathbf{2^{Sc}}$ by the upfield shift of the hydrogen resonances of the 4 and 4′-positions, from 7.20 ppm in free 2,2′-bipyridine (C_6D_6, 25 °C) to 4.08 ppm (4-position, dearomatized ring) and 6.90 ppm (4′-position) in the dearomatized complex. The protons on the 3 and 5-positions showed an upfield shift as well, to the olefinic region of the ^{1}H NMR spectrum: a doublet of doublets at 5.54 ppm (3-position) and a doublet of triplets at 4.76 ppm (5-position) were assigned to these protons (coupling of the C3 and C5 protons occurs). The ^{1}H NMR spectrum of the lutetium product was analogous to that of $\mathbf{2^{Sc}}$. A ^{1}H−^{1}H COSY experiment (25 °C, C_6D_6) was performed on $\mathbf{2^{Lu}}$, confirming the assignments of the ^{1}H NMR spectra (see the Supporting Information for details) and the coupling between the C3 and C5 protons.

X-ray crystallography indicated that the alkyl transfer occurred to the 4-position of one of the pyridine rings to give $\mathbf{2^{M}}$ (Figure 1, M = Sc).[19] It is likely that an initial 1,3-alkyl transfer to the 2-position takes place to give $\mathbf{2^{M}-1,3}$, which is similar to the product of the 1,3-alkyl transfer from $Lu(CH_2SiMe_3)_3(THF)_2$ to terpyridine,[23] and then an isomerization leads to $\mathbf{2^{M}}$, likely to be the thermodynamically stable product. Similar behavior has been reported for the reactions of group 3 hydride complexes with pyridine.[61−65] Metrical parameters were consistent with the dearomatization of one of the pyridine rings. For example, the C−C distances in the aromatic ring are 1.3774(41), 1.3729(44), 1.3841(45), and 1.3961(42) Å, while in the dearomatized one they are 1.3458(44), 1.5008(50), 1.5058(49), and 1.3354(45) Å, with the two longest distances to the sp^3-carbon atom. Also, the Sc−N distance to the dearomatized pyridine ring, 2.1397(25) Å, is shorter by 0.15 Å than the Sc−N distance (2.2827(24) Å) to the aromatic ring. The CCC angles around the sp^3-carbon atom of 107.5(3), 109.89(33), and 110.52(34)° are in agreement with the above structural assignment.

Scheme 2. Reactions of Isoquinoline Mediated by the Benzyl Complexes $\mathbf{1^{M}-THF}$ (*M* = Sc/Y/Lu/La)

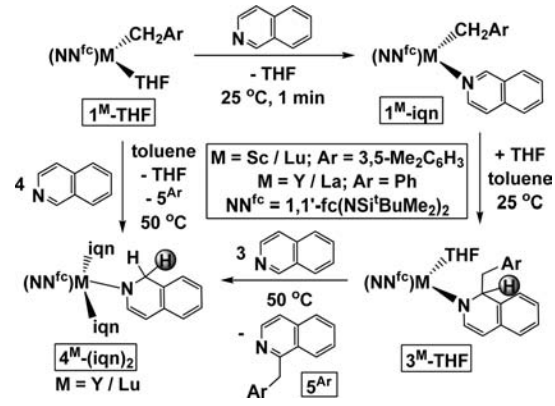

Since the reaction of $\mathbf{1^{Sc}-THF}$ with 8-methylisoquinoline led to the expected ortho-metalated product,[55] a study of the reactivity behavior of the alkyl metal complexes $\mathbf{1^{M}-THF}$ with isoquinoline (iqn) was undertaken next. The reaction of $\mathbf{1^{M}-THF}$ with isoquinoline first led to THF displacement by the N-heterocycle ($\mathbf{1^{M}-iqn}$, Scheme 2). Upon further reaction, the inspection of the ^{1}H NMR spectrum of the product revealed neither free mesitylene nor toluene, which would result from the C−H activation of the heterocycle. Rather, a 1,3-alkyl migration of the benzyl group onto the α-carbon of isoquinoline took place at room temperature (M = Y, Lu, La) or 50 °C (M = Sc), resulting in the formation of $\mathbf{3^{M}-THF}$ (Scheme 2). This migration was accompanied by the appearance in the ^{1}H NMR (500 MHz, C_6D_6) spectrum of the lutetium complex $\mathbf{3^{Lu}-THF}$ (the other complexes show analogous NMR characteristics) of a doublet at 5.98 ppm, as well as a doublet of doublets at 5.20 ppm. The appearance of those signals was concomitant with the disappearance of aromatic isoquinoline peaks. By using deuterium-labeled isoquinoline, in which deuterium incorporation at the 1 and 3-positions was 36 and 54%, respectively, an investigation of the ^{2}H NMR spectrum for the corresponding product was possible. Its examination allowed the assignment of the peak at 5.20 ppm to the C1 proton of the dearomatized isoquinoline as well as the peak at 7.58 ppm to the C3 proton. These assignments were corroborated by an ^{1}H−^{1}H COSY experiment (25 °C, C_6D_6) that revealed that the resonances at 5.98 ppm and 7.58 ppm belong, indeed, to protons on the adjacent C4 and C3 carbons, respectively. The methylene protons of the benzyl group were found at 3.38 and 2.83 ppm as two doublets of doublets that integrated to one proton each. Furthermore, each methylene proton and the C1 proton were found to be related by the ^{1}H−^{1}H COSY experiment. The ^{1}H NMR spectroscopy assignment was confirmed by ^{13}C NMR spectroscopy as well: two peaks, at 108.9 and 98.8 ppm, were assigned to C3 and C4 of isoquinoline, respectively, since those carbons are olefinic. Five sharp peaks were found in the aliphatic region of the spectrum from 40.2 ppm to 20.6 ppm. These peaks were assigned to the methylene carbon, C1 of isoquinoline, the two methyl carbons of the benzyl moiety, and the remaining carbons of the NN^{fc} ligand (see the experimental section for the full assignment).

An X-ray diffraction study of $\mathbf{3^{Lu}-THF}$ confirmed the identity of the product; unfortunately, the data collection was of poor quality and only connectivity information could be

(59) Vidyaratne, I.; Scott, J.; Gambarotta, S.; Duchateau, R. *Organometallics* **2007**, *26*, 3201–3211.
(60) Knijnenburg, Q.; Gambarotta, S.; Budzelaar, P. H. M. *Dalton Trans.* **2006**, 5442–5448.
(61) Evans, W. J.; Meadows, J. H.; Hunter, W. E.; Atwood, J. L. *J. Am. Chem. Soc.* **1984**, *106*, 1291–1300.
(62) Deelman, B.-J.; Stevels, W. M.; Teuben, J. H.; Lakin, M. T.; Spek, A. L. *Organometallics* **1994**, *13*, 3881–3891.
(63) Gountchev, T. I.; Tilley, T. D. *Organometallics* **1999**, *18*, 2896–2905.
(64) Kirillov, E.; Lehmann, C. W.; Razavi, A.; Carpentier, J.-F. *Eur. J. Inorg. Chem.* **2004**, *2004*, 943–945.
(65) Robert, D.; Voth, P.; Spaniol, T. P.; Okuda, J. *Eur. J. Inorg. Chem.* **2008**, *2008*, 2810–2819.

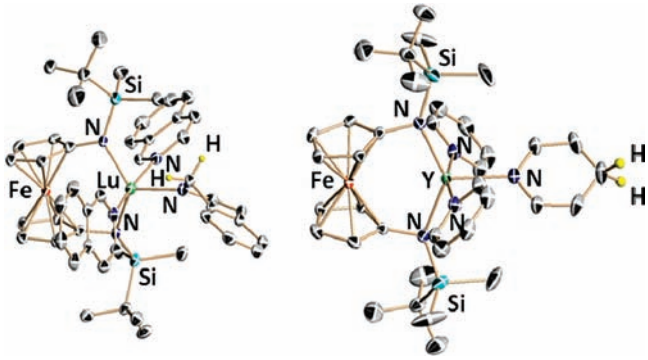

Figure 2. ORTEP representation of $\mathbf{4^{Lu}\text{-}(iqn)_2}$ (left, 50% probability) and $\mathbf{4'^{Y}\text{-}1,5\text{-}(py)_2}$ (right, 35% probability); irrelevant hydrogen atoms were removed for clarity.

gathered. However, the analogous yttrium complex, $\mathbf{3^{Y}-iqn^{Me}}$, in which isoquinoline and THF were replaced by 3-methylisoquinoline (iqn^{Me}), provided good quality data. X-ray crystallography (Figure 1) confirmed that the alkyl transfer occurred to the 1-position of isoquinoline. Although an argument could be construed that for $\mathbf{3^{Y}-iqn^{Me}}$ the 3-position bears the methyl group and, therefore, steric hindrance would prevent transfer of the benzyl group to that position, the NMR spectroscopy data support the preferred transfer to the 1-position for both isoquinoline and 3-methylisoquinoline, as does the connectivity information obtained from the structure of $\mathbf{3^{Lu}-THF}$. Metrical parameters are consistent with the dearomatization of the pyridine ring. For example, the N−C distances in the coordinated isoquinoline are 1.3272(47) and 1.3830(048) Å, while in the dearomatized one they are 1.3761(48) and 1.4693(44) Å, with the longest distance to the sp^3-carbon atom. In addition, C−C distances also reflect the dearomatization of one isoquinoline ligand: the values for the pyridine ring of the coordinated isoquinoline are 1.3990(50), 1.4140(55), 1.3693(52), and 1.4191(52) Å, while in the dearomatized one they are 1.4204(53), 1.5186(51), 1.4395(52), and 1.3690(53) Å, with the longest distance involving the sp^3-carbon atom. The Y−N distance to the dearomatized isoquinoline (2.2770(31) Å) is shorter by almost 0.2 Å than the Y−N distance (2.4675(32) Å) to the aromatic, coordinated one. The angles around the sp^3-carbon atom of CCC − 109.77(28)° and NCC − 110.15(27), 113.08(32)° also support the above structural assignment.

During the course of the reaction of $\mathbf{1^{M}-THF}$ with isoquinoline, it was noticed that employing an excess of the substrate led to the formation of a new product. Consequently, the reaction of three equivalents of isoquinoline with $\mathbf{3^{Y}-THF}$ for six hours or with $\mathbf{3^{Lu}-THF}$ for thirty hours, at 50 °C, allowed the isolation of $\mathbf{4^{M}-(iqn)_2}$ (Scheme 2). The ^{1}H NMR (300 MHz, C_6D_6) spectrum of $\mathbf{4^{Lu}-(iqn)_2}$ showed the appearance of two doublets corresponding to one proton each, at 6.43 and 5.69 ppm, assigned to the C3 and C4 protons, respectively, of the dearomatized isoquinoline ligand. A singlet at 4.56 ppm, which integrated to two protons, was also identified and assigned to the protons on the 1-position of the dearomatized isoquinoline. Integration of the remaining peaks supported the presence of two additional coordinated isoquinoline ligands. The ^{1}H NMR spectrum of the yttrium product was analogous to that of the lutetium one.

The compound $\mathbf{4^{Lu}-(iqn)_2}$ was also characterized by single-crystal X-ray diffraction (Figure 2), which confirmed that two isoquinoline ligands were coordinated in $\mathbf{4^{Lu}-(iqn)_2}$ instead of the one found in $\mathbf{3^{Y}-iqn^{Me}}$. It is likely that less steric crowding

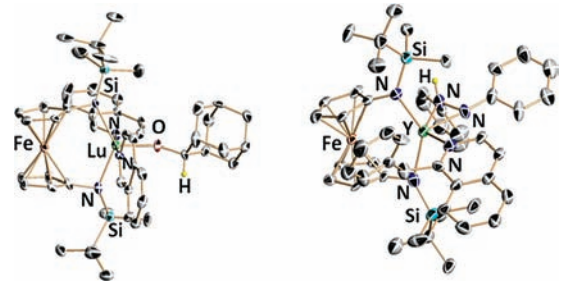

Figure 3. ORTEP representation of $\mathbf{6^{Lu}-(iqn)_2}$ (left) and $\mathbf{8^{Y}}$ (right) with ellipsoids drawn at the 50% probability level (irrelevant hydrogen atoms were removed for clarity).

is present in $\mathbf{4^{Lu}-(iqn)_2}$ because of the absence of the benzyl group in the proximity of the metal center. Metrical parameters are similar to those observed for $\mathbf{3^{Y}-iqn^{Me}}$, with long C−C and N−C distances of 1.5110(40) and 1.4721(36) Å, respectively, and an NCC angle of 113.17(24)° at the sp^3-carbon atom.

Inspection of the crude reaction mixture by ^{1}H NMR spectroscopy revealed that there was a second product present, $\mathbf{5^{Ar}}$ (Scheme 2). The two products, $\mathbf{4^{M}-(iqn)_2}$ and $\mathbf{5^{Ar}}$, were separated by fractional crystallization from hexanes. The comparison of the ^{1}H NMR spectrum of $\mathbf{5^{Ar}}$ with spectra reported for 1-(3,4-dimethylbenzyl)isoquinoline and 1-(4-methylbenzyl)isoquinoline[66] allowed its identification as 1-benzylisoquinoline or 1-(3,5-dimethylbenzyl)isoquinoline. Also, the identity of $\mathbf{5^{Ar}}$, Ar = Ph (1-benzylisoquinoline), was verified by the X-ray crystal structure of another reaction product, in which 1-benzylisoquinoline was coordinated to the metal center (see below, Figure 3).

The mixture of $\mathbf{4^{M}-(iqn)_2}$ and $\mathbf{5^{Ar}}$ can also be accessed directly from the reaction of $\mathbf{1^{M}-THF}$ with four equivalents of isoquinoline. For $\mathbf{4^{M}-(iqn)_2}$ to be produced, a hydrogen must migrate from the benzyl-substituted isoquinoline to one of the coordinated isoquinoline ligands, resulting in the dearomatization of the latter along with the concurrent rearomatization of the former. A hydrogen migration of this type can take place through one of several different mechanisms, which will be discussed below in conjunction with the results from computational studies. After rearomatization, the coordinated $\mathbf{5^{Ar}}$ is likely replaced by isoquinoline.

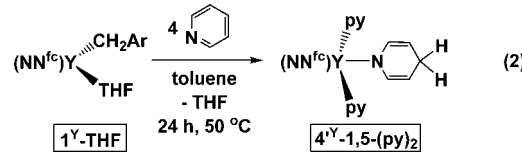

(2)

The reaction of $\mathbf{1^{M}-THF}$ with pyridine has always given a mixture of products that proved intractable. In one instance though, when the yttrium complex $\mathbf{1^{Y}-THF}$ was employed, a product reminiscent of $\mathbf{4^{Y}-(iqn)_2}$ was isolated (eq 2). However, instead of identifying $\mathbf{4'^{Y}-1,3\text{-}(py)_2}$, in which the dearomatized pyridine bears the additional hydrogen atom at the 2-position, as was the case for isoquinoline, the product of the hydrogen migration to the 4-position, $\mathbf{4'^{Y}-1,5\text{-}(py)_2}$, was identified by X-ray crystallography (Figure 2). Unfortunately, this reaction suffered from poor reproducibility and attempts to characterize $\mathbf{4'^{Y}-1,5\text{-}(py)_2}$ by other methods were thwarted by its contamination with other products. As will be discussed in the

(66) Uff, B. C.; Kershaw, J. R. *J. Chem. Soc. (C)* **1969**, 666–668.

Scheme 3. Hydrogen Transfer to Ketones from **3^{M}−THF** (M = Sc/Y/La/Lu)

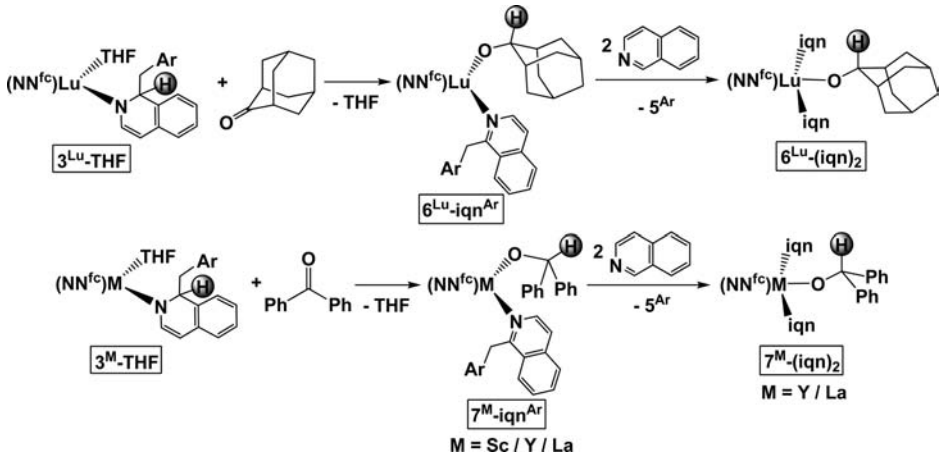

computational-study section, both the alkyl and hydrogen-transfer reactions have high activation barriers that are similar in magnitude in the case of pyridine. Furthermore, the product of the hydrogen-transfer reaction is not as stabilized with respect to the starting material as in the case of isoquinoline. When these considerations are taken into account, along with the possibility that other reactions between **1^{Y}−THF** and pyridine could also occur,[54,55] it is not surprising that the product **4′^{Y}−1,5-(py)$_2$** could not be obtained reproducibly.

It was reasoned that the hydrogen migration from **3^{M}−THF** may also occur in the presence of other substrates. Indeed, the reaction of **3^{M}−THF** with 2-adamantanone or benzophenone led to the formation of new products, **6^{Lu}−iqn^{Ar}** and **7^{M}−iqn^{Ar}** (M = Sc, Y, La), respectively (Scheme 3). Although ^{1}H NMR spectroscopy showed that the alkoxide formation had taken place in the presence of the ketone substrate alone, the addition of two equivalents of isoquinoline was necessary to facilitate the crystallization of the products as **6^{Lu}−(iqn)$_2$** and **7^{M}−(iqn)$_2$** (M = Y, La).

Analysis of the ^{1}H NMR (500 MHz, C_6D_6) spectrum of **6^{Lu}−(iqn)$_2$** showed a new peak at 4.55 ppm corresponding to the hydrogen on the newly sp^3-hybridized carbon, the adamantyl C2. This proton displayed the expected downfield shift relative to the other adamantyl protons, which were located significantly more upfield, in the region from 2.32 to 1.39 ppm. The complexes **7^{M}−(iqn)$_2$** were characterized by ^{1}H and ^{13}C NMR spectroscopy and elemental analysis. Their structural assignment was based upon comparison of their ^{1}H NMR spectra to that of **6^{Lu}−(iqn)$_2$**. X-ray crystallography of **6^{Lu}−(iqn)$_2$** confirmed the solution structure (Figure 3): the Lu−O distance of 2.0368(51) Å is similar to other Lu−O distances in alkoxide complexes.[67−69] Also, the C−O distance of 1.4160(75) Å and the OCC/CCC angles of 111.07(53), 112.97 (0.55), and 108.11(52)° involving the former ketone carbon are consistent with the presence of an sp^3-hybridized carbon atom.

Another substrate used to probe the hydrogen transfer from **3^{M}−THF** was azobenzene. The reaction between **3^{Y}−THF** and azobenzene gave the product **8^{Y}**, in which a hydrogen atom had been transferred from the dearomatized 1-benzylisoquinoline moiety to one of the nitrogen atoms of azobenzene (eq 3). The single-crystal X-ray structure of **8^{Y}** (Figure 3) allowed the unambiguous assignment of 1-benzylisoquinoline, formed by the rearomatization of the N-heterocyclic fragment, as mentioned earlier. Furthermore, the metrical parameters of the newly formed hydrazide fragment are consistent with the reduction of azobenzene: the N−N distance of 1.4626(61) Å is similar to N−N distances in other [η^2-(PhNH−NPh)]$^-$ complexes,[70−72] while the Y−N distances are significantly different from each other (2.2525(48) and 2.4359(45) Å).

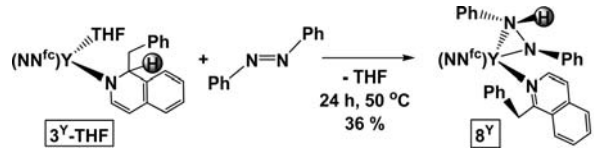

(3)

Since different types of mechanisms can be envisioned for the hydrogen transfer, β-hydride elimination and direct transfer from one ligand to another (see below), it was reasoned that if hydride transfer operates then it should also occur to nonpolar substrates, such as alkenes and alkynes.[73] Therefore, reactions of **3^{M}−THF** with 2-butyne, diphenylacetylene, and ethylene were carried out. Initially, a transformation of the starting material was observed, but since the same outcome was identified in all of those reactions, it was reasoned that no reaction took place with any of the substrates. Indeed, when **3^{M}−THF** was heated in C_6D_6 by itself (eq 4), the previous reaction mixture was also obtained. Interestingly, either toluene (M = Y, La) or mesitylene (M = Sc, Lu) was produced as a byproduct in the reaction, suggesting a possible β-alkyl elimination of the benzyl moiety as a reaction pathway. β-Alkyl elimination on group 3 metals is not without precedent and is as common as β-hydride elimination as a decomposition pathway for organo-f-element complexes.[74,75] However, inspection of the ^{2}H NMR spectrum of the reaction products showed

(67) Konkol, M.; Spaniol, T. P.; Kondracka, M.; Okuda, J. *Dalton Trans.* **2007**, 4095–4102.
(68) Anwander, R.; Munck, F. C.; Priermeier, T.; Scherer, W.; Runte, O.; Herrmann, W. A. *Inorg. Chem.* **1997**, *36*, 3545–3552.
(69) Beer, P. D.; Drew, M. G. B.; Kan, M.; Leeson, P. B.; Ogden, M. I.; Williams, G. *Inorg. Chem.* **1996**, *35*, 2202–2211.
(70) Yuan, F. *Synth. React. Inorg. ME* **2005**, *35*, 703–708.
(71) Evans, W. J.; Kociok-Koehn, G.; Leong, V. S.; Ziller, J. W. *Inorg. Chem.* **1992**, *31*, 3592–3600.
(72) Zambrano, C. H.; Fanwick, P. E.; Rothwell, I. P. *Organometallics* **1994**, *13*, 1174–1177.
(73) Burger, B. J.; Thompson, M. E.; Cotter, W. D.; Bercaw, J. E. *J. Am. Chem. Soc.* **1990**, *112*, 1566–1577.
(74) Watson, P. L.; Roe, D. C. *J. Am. Chem. Soc.* **1982**, *104*, 6471–6473.
(75) Jeske, G.; Lauke, H.; Mauermann, H.; Swepston, P. N.; Schumann, H.; Marks, T. J. *J. Am. Chem. Soc.* **1985**, *107*, 8091–8103.

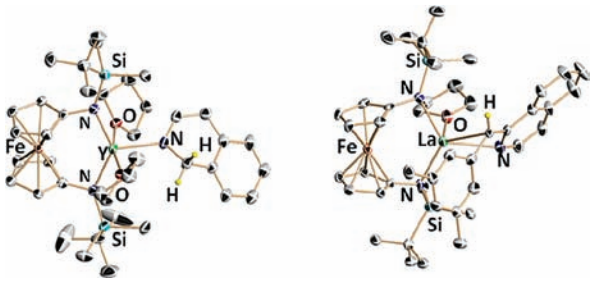

Figure 4. ORTEP representation of $\mathbf{4^{Y}-(THF)_2}$ (left) and $\mathbf{9^{La}}$ (right) with ellipsoids drawn at the 50% probability level (irrelevant hydrogen atoms were removed for clarity).

that the toluene/mesitylene observed did not contain deuterium, so the deuterated solvent was not involved in its formation.

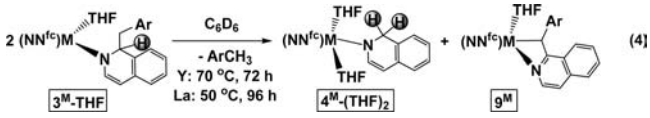

The workup of the reaction mixture revealed that two products, $\mathbf{4^{M}-(THF)_2}$ and $\mathbf{9^{M}}$, were formed in a 1:1 ratio (eq 4). The two products were separated by fractional crystallization giving red and orange crystals. Because of differing solubility properties, the orange crystals were characterized by X-ray crystallography for the yttrium complex and the red crystals for the lanthanum one. For scandium and lutetium, analogous reaction mixtures were formed based on their ^{1}H NMR spectra, but the products could not be isolated. X-ray crystallography indicated that the orange crystals corresponded to $\mathbf{4^{Y}-(THF)_2}$, while the red ones to $\mathbf{9^{La}}$ (Figure 4). The reaction stoichiometry is wrong for the number of THF molecules involved, but it is possible that an additional molecule of THF is necessary only during the crystallization of $\mathbf{4^{M}-(THF)_2}$ and the decomposition of $\mathbf{9^{M}}$ may provide it. The X-ray crystal structure of $\mathbf{4^{Y}-(THF)_2}$ is similar to that of $\mathbf{4^{Lu}-(iqn)_2}$, with long C−C and N−C distances of 1.5092(47) and 1.4749(41) Å, respectively, and an NCC angle of 112.79(28)° at the sp^3-carbon atom. The X-ray crystal structure of $\mathbf{9^{La}}$ shows the formation of a lanthanum pseudo-η^3-allyl fragment and the rearomatization of the pyridine ring; the La−C_{allyl} distances of 2.8832(55), 2.9489(53), and 3.0622(55) Å and La−N_{iqn} distance of 2.5827(44) Å are consistent with this formulation. It is proposed that the longer La−C_{allyl} distances than those found in other lanthanum-allyl complexes[76−81] are a consequence of the charge delocalization over four bonds to include the N−C bond of the isoquinoline fragment. This delocalization is supported by the shorter La−N_{iqn} distance than those found in other lanthanum-pyridine complexes.[82−84] The two C−C distances of 1.4032(71) and 1.4687(73) Å and the N−C distance of 1.3720(65) Å are consistent with this interpretation.

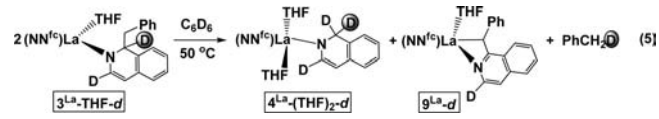

It is likely that two molecules of $\mathbf{3^{M}-THF}$ are required to form the two reaction products $\mathbf{4^{M}-(THF)_2}$ and $\mathbf{9^{M}}$. Although an in-depth mechanistic study of this process is beyond the scope of the present article, the reaction of $\mathbf{3^{La}-THF}$-***d*** (for the formation of $\mathbf{3^{La}-THF}$-***d***, isoquinoline deuterated at the 1−36% and 3−54% positions was used) showed the formation of deuterated toluene (eq 5). The integration of the methyl-deuterons from the toluene obtained (ca. 30%) was consistent with toluene formation from the benzyl and the deuteron on the C1 carbon, but given that a substrate that was 100% deuterium labeled at this position could not be obtained, other possibilities cannot be excluded. The reaction in eq 4 is somewhat similar to that reported by Cronin et al. for phenanthridinium salts:[85] in the presence of amines, the phenanthridinium salt was dearomatized and a product corresponding to $\mathbf{3^{M}-THF}$ was formed. In the presence of a base, the dearomatized phenanthridinium transferred one proton to a molecule of the initial phenanthridinium salt, leading to the formation of a product corresponding to $\mathbf{4^{M}-(THF)_2}$, and underwent rearomatization, giving a product corresponding to $\mathbf{9^{M}}$.

It was observed that the reaction in eq 4 was faster for the lanthanum complex than for the yttrium one, an observation supporting the proposal that the reaction is bimolecular in nature. The larger lanthanum center would allow the two coordination spheres to come into closer proximity than the yttrium one would. Another factor that may influence the outcome of the reaction is the fact that both the yttrium and lanthanum complexes $\mathbf{3^{M}-THF}$ liberate toluene, while the scandium and lutetium complexes eliminate mesitylene. It is possible that the electron-donating properties of the two methyl groups disfavor the formation of mesitylene. Other factors may also be responsible, given the complex nature of the reaction outcome.

Computational Studies. Calculations at the B3LYP/LACV3P++**(2f) level were performed to gain insight into different pathways for the reactions studied. For consistency, all calculations employed yttrium complexes, using the full NN^{fc} ligand. First, the electronic nature of the benzyl transfer from yttrium to the 2-position of pyridine (to simplify computer effort) was investigated (Scheme 4a) as a model for the transformation $\mathbf{1^{Y}-THF}$ to $\mathbf{3^{Y}-THF}$ (Scheme 2). By using one molecule of pyridine as a model substrate, the barrier for alkyl transfer for $\mathbf{1^{Y}-py}$ was found to be 29.8 kcal/mol (Scheme 4a). When an additional molecule of pyridine was coordinated to the yttrium center, the barrier for alkyl transfer was slightly lower, at 25.4 kcal/mol (Scheme 4b), than in the previous case, and the transformation led to $\mathbf{3'^{Y}-py}$, which was 12.3 kcal/mol more stable than $\mathbf{3'^{Y}}$. An extra molecule of pyridine lowered the

(76) Kretschmer, W. P.; Brummelhuis, B. t.; Meetsma, A.; Teuben, J. H. *Z. Anorg. Allg. Chem.* **2006**, *632*, 1933–1935.
(77) Karsch, H. H.; Appelt, A.; Müller, G. *Angew. Chem., Int. Ed.* **1986**, *25*, 823–824.
(78) Taube, R.; Windisch, H.; Hemling, H.; Schumann, H. *J. Organomet. Chem.* **1998**, *555*, 201–210.
(79) Taube, R.; Windisch, H.; Görlitz, F. H.; Schumann, H. *J. Organomet. Chem.* **1993**, *445*, 85–91.
(80) Taube, R.; Windisch, H.; Weienborn, H.; Hemling, H.; Schumann, H. *J. Organomet. Chem.* **1997**, *548*, 229–236.
(81) Taube, R.; Windisch, H.; Maiwald, S.; Hemling, H.; Schumann, H. *J. Organomet. Chem.* **1996**, *513*, 49–61.
(82) Giesbrecht, G. R.; Collis, G. E.; Gordon, J. C.; Clark, D. L.; Scott, B. L.; Hardman, N. J. *J. Organomet. Chem.* **2004**, *689*, 2177–2185.
(83) Katkova, M. A.; Kurskii, Y. A.; Fukin, G. K.; Averyushkin, A. S.; Artamonov, A. N.; Vitukhnovsky, A. G.; Bochkarev, M. N. *Inorg. Chim. Acta* **2005**, *358*, 3625–3632.
(84) Giesbrecht, G. R.; Gordon, J. C.; Clark, D. L.; Scott, B. L. *Appl. Organomet. Chem.* **2005**, *19*, 98–99.
(85) Parenty, A. D. C.; Smith, L. V.; Pickering, A. L.; Long, D.-L.; Cronin, L. *J. Org. Chem.* **2004**, *69*, 5934–5946.
(86) Tsuruta, H.; Yamaguchi, K.; Imamoto, T. *Chem. Commun.* **1999**, 1703–1704.

Scheme 4. Potential Free Energies (Δ*G*) at 298 K for the Alkyl Transfer from (a) **1^{Y}−py** to **3′^{Y}** and (b) **1^{Y}−(py)$_2$** to **3′^{Y}−py**, Showing Selected Bond Distances for the Transition Structure **1TS3′^{Y}−(py)$_2$**

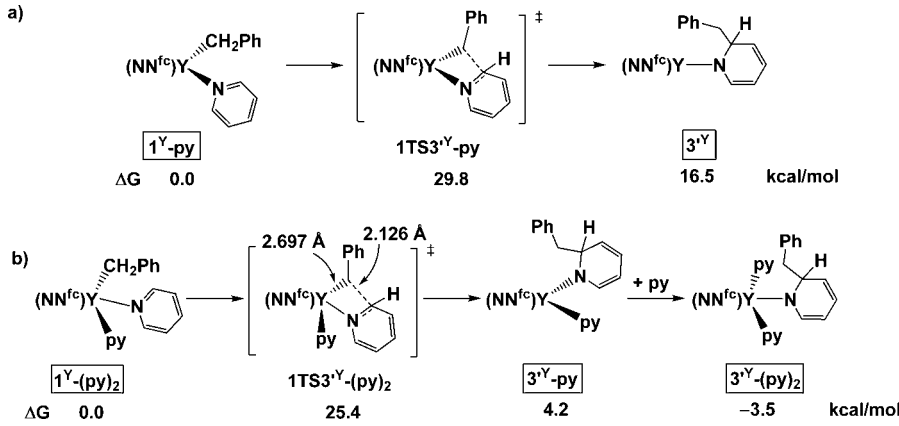

Scheme 5. Proposed Mechanisms for the Transformation of **3^{M}−THF** to **4^{M}−(iqn)$_2$**

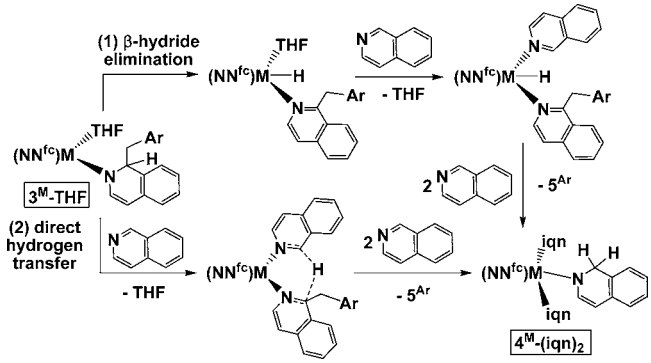

energy of the product further, by 7.7 kcal/mol, consistent with the experimental observations, since the isolated complexes were analogous to **3′^{Y}−(py)$_2$**.

In order to understand the details of the alkyl-transfer reaction, a natural bond orbital analysis on **1TS3′^{Y}−(py)$_2$** was performed. A negative charge buildup was observed at the migrating benzyl carbon (−0.68) and at the N atom (−0.77) of the heterocycle undergoing dearomatization. The natural localized molecular orbital/natural population analysis[87,88] bond orders showed a bond order of 0.08 for Y−C^{Bz} (2.697 Å distance) and a bond order of 0.55 for C^{Bz}−C^{py} (2.126 Å distance). These values indicate a late transition state where the benzyl carbon migrates as a carbanion and has almost completely detached from yttrium, while the receiving pyridine is partially dearomatized at the potential energy saddle point. Our results suggest that the activation barriers in the dearomatization of heterocycles will likely correlate with the lost aromatic stabilization energy.[89]

Next, the transformation from **3^{M}−THF** to **4^{M}−(iqn)$_2$** (Scheme 2) was studied. Two types of mechanisms were envisioned (Scheme 5): (1) *β*-hydride elimination and (2) direct transfer from one heterocyclic ligand to another. Both types of mechanisms have been proposed to explain the Meerwein−Ponndorf−Verley reduction of ketones by various metal catalysts,[90−104] a reaction similar to the transformation of **3^{M}−iqn** to **4^{M}−(iqn)$_2$**. In addition to the two mechanisms considered by us, a radical mechanism had also been proposed for the Meerwein-Ponndorf-Verley reduction of ketones.[105] The first mechanism, the hydridic route, is often invoked when explaining the behavior of transition metal catalysts and involves the formation of a metal hydride followed by hydride transfer from the metal to the substrate.[106−108] The second mechanism, the direct-hydrogen transfer, used mostly for aluminum-group complexes, implies a concerted-hydrogen transfer, where both the hydrogen donor and the hydrogen acceptor are held in close proximity by the metal center, and involves a cyclic transition state. Recently, a combined computational and experimental study presented evidence supporting the direct hydrogen-transfer mechanism for catalysis by aluminum complexes.[104]

(87) Reed, A. E.; Curtiss, L. A.; Weinhold, F. *Chem. Rev.* **1988**, *88*, 899–926.
(88) Glendening, E. D.; Badenhoop, J. K.; Reed, A. E.; Carpenter, J. E.; Bohmann, J. A.; Morales, C. M.; Weinhold, F. *NBO. Version 5.0*; Theoretical Chemistry Institute, University of Wisconsin: Madison, WI, 2001.
(89) Mandado, M.; Otero, N.; Mosquera, R. A. *Tetrahedron* **2006**, *62*, 12204–12210.
(90) Meerwein, H.; Schmidt, R. *Liebigs Ann. Chem.* **1925**, *444*, 221–238.
(91) Ponndorf, W. *Angew. Chem.* **1926**, *39*, 138–143.
(92) Verley, M. *Bull. Soc. Chim. Fr.* **1925**, 871–874.
(93) Cha, J. S. *Org. Proc. Res. Dev.* **2006**, *10*, 1032–1053.
(94) de Graauw, C. F.; Peters, J. A.; van Bekkum, H.; Huskens, J. *Synthesis* **1994**, *1994*, 1007–1017.
(95) Yan, P.; Nie, C.; Li, G.; Hou, G.; Sun, W.; Gao, J. *Appl. Organomet. Chem.* **2006**, *20*, 338–343.
(96) Fukuzawa, S.-i.; Nakano, N.; Saitoh, T. *Eur. J. Org. Chem.* **2004**, *2004*, 2863–2867.
(97) Klomp, D.; Maschmeyer, T.; Hanefeld, U.; Peters, J. A. *Chem.−Eur. J.* **2004**, *10*, 2088–2093.
(98) Nakano, Y.; Sakaguchi, S.; Ishii, Y. *Tetrahedron Lett.* **2000**, *41*, 1565–1569.
(99) Nishikido, J.; Yamamoto, F.; Nakajima, H.; Mikami, Y.; Matsumoto, Y.; Mikami, K. *Synlett* **1999**, *1999*, 1990–1992.
(100) Evans, D. A.; Nelson, S. G.; Gagne, M. R.; Muci, A. R. *J. Am. Chem. Soc.* **2002**, *115*, 9800–9801.
(101) Lebrun, A.; Namy, J.-L.; Kagan, H. B. *Tetrahedron Lett.* **1991**, *32*, 2355–2358.
(102) Namy, J. L.; Souppe, J.; Collin, J.; Kagan, H. B. *J. Org. Chem.* **1984**, *49*, 2045–2049.
(103) Fernandez, I.; Sierra, M. A.; Cossio, F. P. *J. Org. Chem.* **2007**, *72*, 1488–1491.
(104) Cohen, R.; Graves, C. R.; Nguyen, S. T.; Martin, J. M. L.; Ratner, M. A. *J. Am. Chem. Soc.* **2004**, *126*, 14796–14803.
(105) Ashby, E. C. *Acc. Chem. Res.* **1988**, *21*, 414–421.
(106) Zassinovich, G.; Mestroni, G.; Gladiali, S. *Chem. Rev.* **1992**, *92*, 1051–1069.
(107) Hanasaka, F.; Fujita, K.-i.; Yamaguchi, R. *Organometallics* **2004**, *23*, 1490–1492.
(108) Kitamura, M.; Tsukamoto, M.; Bessho, Y.; Yoshimura, M.; Kobs, U.; Widhalm, M.; Noyori, R. *J. Am. Chem. Soc.* **2002**, *124*, 6649–6667.

β-Hydride elimination is not common for group 3 metals, although it can take place.[109−112] Past studies have found that, in general, β-hydride elimination mechanisms for lanthanide and actinide metal complexes would be much more endothermic than their counterparts in the late transition metals.[113] The lack of reactivity toward olefins and alkynes points to the direct hydrogen transfer as being the viable route. Accordingly, when the β-hydride elimination pathway was evaluated, no saddle point on the pathway where the hydrogen was transferred from the ligand to yttrium was found. All attempts led to a stepwise process, where the acidic hydrogen detached first, leading to rearomatization of the heterocycle, followed by the formation of an yttrium hydride species, with an activation barrier of ∼56 kcal/mol in toluene. The large activation barrier is not surprising since the migrating hydrogen carries a partial positive charge (as a consequence of the nature of the rearomatization process) while the metal is also positively charged (+2.0).

In the case of the direct transfer pathway to the 2-position of pyridine, a transition state was found at 25.2 kcal/mol starting from $\mathbf{3'^{Y}-(py)_2}$ and leading to $\mathbf{4'^{Y}-(py)_2}$, which was 6.2 kcal lower in energy than $\mathbf{3'^{Y}-(py)_2}$ (Scheme 6a). Given that an analagous product to $\mathbf{4'^{Y}-1,5\text{-}(py)_2}$ was observed experimentally, a pathway for the direct transfer to the 4-position of pyridine was also studied and was found to have an activation barrier 15.4 kcal/mol higher in energy than that calculated for the transfer to the 2-position, albeit the products were virtually isoenergetic. The value of 40.6 kcal/mol for the direct transfer to the 4-position suggests that the transfer to the 2-position is likely to occur first, giving $\mathbf{4'^{Y}-(py)_2}$, which possibly isomerizes to $\mathbf{4'^{Y}-1,5\text{-}(py)_2}$.

It was anticipated that the barrier for the direct transfer from pyridine to isoquinoline would be considerably lower than for pyridine-to-pyridine transfer because the relative magnitude of the lost (aza-ring in isoquinoline) versus regained (pyridine) aromatic stabilization energy is higher for pyridine than for isoquinoline (the total aromatic stabilization energy for isoquinoline is higher than that for pyridine, however, the aromatic stabilization energy of the N-containing ring of isoquinoline is lower than that of pyridine).[89] In order to evaluate this, the direct transfer from a dearomatized benzylpyridine to isoquinoline was studied. It was found that the activation barrier was indeed much lower than for the pyridine case (only 13.0 kcal/mol versus the starting material).

The direct transfer from isoquinoline to isoquinoline (Scheme 6c) was also studied: a barrier of 20.6 kcal/mol was found, consistent with a six-hour reaction time at 50 °C. In addition, our hypothesis, that the energetic profile of H-transfer is dependent on the net aromatic stabilization energy, was supported by the relative free energies (ΔG) of the three reactions analyzed (Scheme 6): transformations where both reacting heterocycles were the same (small changes in the aromatic stabilization energy, Scheme 6a and 6c) were less exergonic (−6.2 and −4.2 kcal/mol, respectively) than the reaction where the participating heterocycles were different and there was a gain in the aromatic stabilization energy (−16.5 kcal/mol in the case of H-transfer from pyridine to isoquinoline, Scheme 6b).

Scheme 6. Potential Free Energies (ΔG) at 298 K for the (a) Pyridine-to-Pyridine, (b) Pyridine-to-Isoquinoline, and (c) Isoquinoline-to-Isoquinoline H-Transfer, Displaying the Natural Charge on the N Atoms of the Heterocycles and on the Migrating H Atom (b)

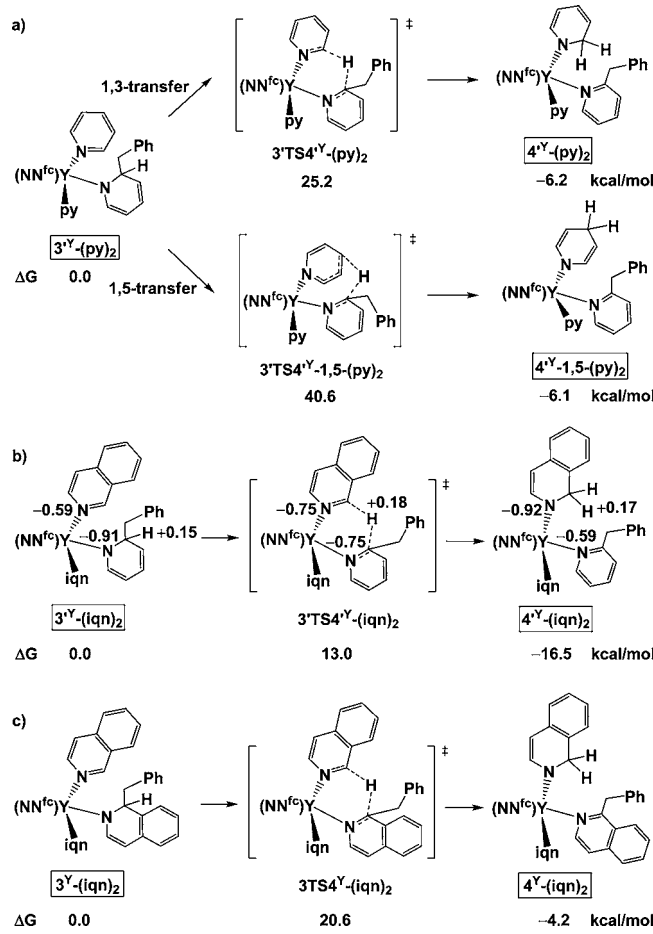

Natural population analyses[87,88] on the N atom of both reacting heterocycles showed an inverted charge profile for each reaction. The charges at the N atom on the isoquinoline ligand changed from −0.59 in $\mathbf{3'^{Y}-(iqn)_2}$, to −0.75 in the transition state $\mathbf{3'TS4'^{Y}-(iqn)_2}$, and −0.92 in $\mathbf{4'^{Y}-(iqn)_2}$ (Scheme 6b), while the charges at the N atom on the substituted pyridine ligand varied in the reverse order (−0.91, −0.75, and −0.59, respectively). The charge at the migrating H was almost constant from +0.15 in $\mathbf{3'^{Y}-(iqn)_2}$, to +0.18 in the transition structure, and +0.17 in $\mathbf{4'^{Y}-(iqn)_2}$; the charge of the metal center underwent a negligible change (∼0.01 e) throughout the transformation. All these data suggest that the hydrogen atom migrates more as a proton than as a hydride, while a significant electronic reorganization is happening at both ligands that, however, does not affect their bonding with the metal center. The reacting ligands were localized at the transition structure in a displaced face-to-face arrangement with the H atom at 1.32 Å from the benzylpyridine carbon and 1.49 Å from the isoquinoline carbon, resembling a chairlike, six-member metalocycle (see the Supporting Information for details).

Conclusions

The reactivity behavior of the benzyl complexes $\mathbf{1^{M}-THF}$ toward 2,2′-bipyridine (M = Sc, Lu) and isoquinoline (M = Sc, Y, Lu, La) was investigated. The observed alkyl transfer to

(109) Ephritikhine, M. *Chem. Rev.* **1997**, *97*, 2193–2242.
(110) Watson, P. L. *J. Am. Chem. Soc.* **1982**, *104*, 337–339.
(111) Evans, W. J.; Meadows, J. H.; Wayda, A. L.; Hunter, W. E.; Atwood, J. L. *J. Am. Chem. Soc.* **1982**, *104*, 2015–2017.
(112) Bazan, G. C.; Schaefer, W. P.; Bercaw, J. E. *Organometallics* **1993**, *12*, 2126–2130.
(113) Bruno, J. W.; Marks, T. J.; Morss, L. R. *J. Am. Chem. Soc.* **1983**, *105*, 6824–6832.

these substrates is in contrast to ortho-metalation reactions reported for a variety of other substituted pyridines and metal complexes. In addition, the products of the 1,3-alkyl-transfer reaction to isoquinoline undergo subsequent transformations. The reactions with polar (isoquinoline, ketones, azobenzene) and nonpolar (olefins, alkynes) unsaturated substrates were investigated and it was found that a hydrogen transfer occurred from the dearomatized isoquinoline ring to polar unsaturated substrates. Olefins and alkynes did not react and, instead, a disproportionation reaction of the dearomatized, benzyl-substituted isoquinoline complexes **3^{M}−THF** was observed. Both types of reactions, the alkyl transfer to isoquinoline and the hydrogen transfer from one isoquinoline to another, were investigated computationally. It was found that the hydrogen transfer occurred through a concerted mechanism akin to that proposed for the Meerwein−Ponndorf−Verley reduction of ketones by aluminum alkoxide complexes. The reactions reported herein add to and contrast the list of reactions observed for group 3 alkyl complexes with aromatic N-heterocycles, a statement of the rich reactivity behavior of these metal centers when they are supported by a ferrocene diamide ligand.

Experimental Section

All experiments were performed under a dry nitrogen atmosphere using standard Schlenk techniques or an MBraun inert-gas glovebox. Solvents were purified using a two-column solid-state purification system by the method of Grubbs[114] and transferred to the glovebox without exposure to air. NMR solvents were obtained from Cambridge Isotope Laboratories, degassed, and stored over activated molecular sieves prior to use. Scandium, yttrium, and lutetium oxides were purchased from Stanford Materials Corporation, 4 Meadowpoint, Aliso Viejo, CA 92656, and used as received. $LaBr_3$, $K(CH_2Xy\text{-}3,5)$, KCH_2Ph, $La(CH_2C_6H_5)_3(THF)_3$,[115] **1^{Sc}−THF**, **1^{Y}−THF**, and **1^{Lu}−THF** were prepared following published procedures.[51,56] The aromatic heterocycles were distilled or recrystallized before use; deuterium-labeled isoquinoline was synthesized by modifying a literature procedure.[116] All other materials were used as received. ^{1}H NMR spectra were recorded on Bruker300, Bruker500, or Bruker600 spectrometers (work supported by the NSF grants CHE-9974928 and CHE-0116853) at room temperature in C_6D_6 unless otherwise specified. Chemical shifts are reported with respect to internal solvent, 7.16 ppm (C_6D_6). CHN analyses were performed by UC Berkeley Micro-Mass facility, 8 Lewis Hall, College of Chemistry, University of California, Berkeley, CA 94720 and by Midwest Microlab, LLC, 7212 N. Shadeland Avenue, Suite 110, Indianapolis, IN 46250.

Synthesis of $La(CH_2\text{-}3,5\text{-}Me_2C_6H_3)_3(THF)_3$, $La(CH_2Ar)_3(THF)_3$. A slurry of $LaBr_3(THF)_3$ (1.5 g, 2.52 mmol) in 1: 1 THF: hexanes (50 mL) was cooled to −78 °C and 2.4 equiv of KCH_2Ar (0.958 g, 6.05 mmol) was added as a solid. The reaction mixture was warmed to 0 °C and stirred for 3 h. The pale yellow slurry was filtered through Celite and the solvent was removed under vacuum. The resulting reddish-orange, oily solid was dissolved in THF and layered with pentane. Yield: 0.676 g, 38% as yellow crystals from THF: *n*-pentane. ^{1}H NMR (500 MHz, C_4D_8O): δ, ppm: 5.96 (s, 3H, *p*-C_6H_3), 5.74 (s, 6H, *o*-C_6H_3), 3.54 (br s, 4H, OCH_2CH_2), 2.02 (s, 18H, C_6H_3-$(CH_3)_2$), 1.69 (br s, 4H, OCH_2CH_2), 1.47 (s, 6H, CH_2). ^{13}C NMR (126 MHz, C_4D_8O): δ, ppm: 151.8, 139.9, 129.1, 119.6, 118.1, 68.2, 26.4, 22.1. Anal. (%) for $C_{39}H_{57}LaO_3$ Calcd: C, 65.71; H, 8.06; N, 0; Found: C, 65.37; H, 8.14; N, <0.2.

Synthesis of 1′^{La}−THF. $La(CH_2Ar)_3(THF)_3$ (600 mg, 0.849 mmol) was divided into two equal portions and each was dissolved in 1: 1 THF: Et_2O (8 mL) and cooled to −35 °C. Each solution was combined with 1 equiv of $fc(NHSi^tBuMe_2)_2$ (190 mg each, 0.850 mmol total), as a cooled solution in Et_2O and stirred for 3 h at 0 °C. The solvent was removed under vacuum, the resulting orange solid was washed with hexanes (0.5 mL), extracted with a 1:1 solution of toluene: hexanes, and filtered through Celite. The volatiles were removed under vacuum, the resulting solid was dissolved in a minimum amount of Et_2O that was layered with *n*-pentane, and the solution was placed in a −35 °C freezer. The product was collected as crystals by decanting the mother liquor. Yield: 600 mg, 92.3%. ^{1}H NMR (500 MHz, C_6D_6): δ, ppm: 6.36 (s, 2H, o-C_6H_2), 6.10 (s, 1H, p-C_6H), 4.01 (br s, 4H, fc-C*H*), 3.71 (br s, 4H, OCH_2CH_2), 3.23 (s, 4H, fc-C*H*), 2.60 (s, 2H, La−CH_2), 2.17 (s, 6H, C_6H_3-$(CH_3)_2$), 1.35 (br s, 4H, OCH_2CH_2), 0.99 (s, 18H, $SiC(CH_3)_3$), 0.18 (s, 12H, $Si(CH_3)_2$). ^{13}C NMR (126 MHz, C_6D_6): δ, ppm: 154.1, 142.6, 118.6, 118.1, 106.5, 70.3, 66.8, 65.7, 65.0, 27.5, 25.4, 22.3, 20.3, −2.9. Anal. (%) for $C_{35}H_{59}FeLaN_2OSi_2$ Calcd: C, 54.40; H, 7.43; N, 3.60; Found: C, 54.29; H, 7.62; N, 3.70.

Synthesis of 1^{La}−THF. 1^{La}−THF was prepared analogously to the preparation of **1′^{La}−THF**, using $La(CH_2C_6H_5)_3(THF)_3$: $La(CH_2C_6H_5)_3(THF)_3$ (1.236 g, 1.97 mmol) was divided in 4 equal portions, dissolved in a 1:1 mixture of THF/Et_2O (8 mL) and cooled to −35 °C. This solution was combined with 1 equiv of $H_2(NN^{fc})$ (219 mg each, 1.97 mmol total), as a cooled solution in Et_2O and stirred for 3 h at 0 °C. The solvent was removed under vacuum, the resulting orange solid was washed with hexanes (1.5 mL), extracted with a 1:1 solution of toluene: hexanes, and filtered through Celite. The volatiles were removed, the solid was dissolved in a minimum amount of Et_2O that was layered with *n*-pentane and the solution was placed in a −35 °C freezer. The product was collected as crystals by decanting the mother liquor. Yield: 950 mg, 64.8% as two crops of crystals. ^{1}H NMR (500 MHz, C_6D_6): δ, ppm: 7.14 (m, 2H, C_6H_5), 6.65 (d, 2H, C_6H_5), 6.32 (t, 1H, C_6H_5), 4.02 (s, 4H, fc-C*H*), 3.63 (br s, 4H, OCH_2CH_2), 3.20 (s, 4H, fc-C*H*), 2.65 (s, 2H, La−CH_2), 1.31 (br s, 4H, OCH_2CH_2), 0.99 (s, 18H, $SiC(CH_3)_3$), 0.15 (s, 12H, $Si(CH_3)_2$).

Synthesis of 2^{Sc}. 1^{Sc}−THF (200 mg, 0.295 mmol) was dissolved in toluene (10 mL) and 1.3 equiv of 2,2′-bipyridine (60 mg, 0.383 mmol) was added as a solid. The reaction mixture turned dark brown immediately and was allowed to stir for 1 h at room temperature. The solvent was removed under vacuum and the resulting brown solid was washed with hexanes, extracted with toluene, and filtered through Celite, and the solvent was removed under vacuum. Yield: 198.8 mg, 80.8% as a solid obtained after toluene removal. ^{1}H NMR (500 MHz, C_6D_6): δ, ppm: 8.52 (d, 1H, bipy 6′-*H*), 7.40 (d, 1H, bipy 3′-*H*), 7.06 (s, 2H, *o*-C_6H_3), 6.90 (t, 1H, bipy 4′-*H*), 6.83 (s, 1H, *p*-C_6H_3), 6.61 (d, 1H, bipy 6-*H*), 6.46 (t, 1H, bipy 5′-*H*), 5.54 (dd, 1H, bipy 3-*H*), 4.77 (dt, 1H, bipy 5-*H*), 4.25−4.22 (m, 2H, fc-C*H*), 4.08 (m, 2H, fc-C*H*), 4.08 (m, 1H, bipy 4-*H*), 4.06 (br s, 4H, OCH_2CH_2), 3.53 and 3.52 (s, 1H, fc-C*H*), 3.14 (s, 2H, fc-C*H*), 3.10 (t, 2H, CH_2-Ar), 2.23 (s, 6H, C_6H_3-$(CH_3)_2$), 1.29 (br s, 4H, OCH_2CH_2), 0.93 and 0.90 (s, 9H, $SiC(CH_3)_3$), 0.41, 0.32, −0.24, and −0.26 (s, 3H, $Si(CH_3)_2$).^{13}C NMR (126 MHz, C_6D_6): δ, ppm: 156.3, 143.7, 142.9, 138.4, 135.9, 135.7, 135.3, 133.8, 127.4, 126.4, 123.7, 118.6, 117.6, 101.9, 99.2, 99.1, 97.1, 70.8, 66.7, 66.6, 66.0, 65.9, 64.3, 64.2, 63.7, 63.6, 47.9, 36.1, 26.0, 25.9, 22.9, 19.6, 19.5, 18.6, 18.5, −4.7, −4.8, −5.1, −5.3. Anal. (%) for $C_{45}H_{65}FeN_4OScSi_2$ Calcd: C, 67.36; H, 7.93; N, 6.04; Found: C, 67.40; H, 8.31; N, 6.16.

Synthesis of 2^{Lu}. 1^{Lu}−THF (107.4 mg, 0.133 mmol) and 1 equiv of 2,2′-bipy (20.7 mg, 0.133 mmol) were dissolved in toluene (6 mL). The dark-brown solution was heated and stirred in a Schlenk flask for 2 d at 85 °C. The solvent was removed by vacuum. The dark-brown solid was then taken up in hexanes and filtered through a fiber-glass filter. The solution was concentrated under vacuum and stored at −35 °C to afford brown crystals. A second crop of crystals was also obtained from the mother liquor in the same manner. Yield: 104.2 mg, 81.3%. ^{1}H NMR (600 MHz, C_6D_6): 8.43

(114) Pangborn, A. B.; Giardello, M. A.; Grubbs, R. H.; Rosen, R. K.; Timmers, F. J. *Organometallics* **1996**, *15*, 1518–1520.
(115) Bambirra, S.; Meetsma, A.; Hessen, B. *Organometallics* **2006**, *25*, 3454–3462.
(116) Calf, G. E.; Garnett, J. L. *J. Phys. Chem.* **1964**, *68*, 3887–3889.

(d, 1H, bipy 6′-*H*), 7.43 (d, 1H, bipy 3′-*H*), 7.05 (s, 2H, *o*-C_6H_3), 6.90 (t, 1H, bipy 4′-*H*), 6.83 (s, 1H, *p*-C_6H_3) 6.53 (d, 1H, bipy 6-*H*), 6.51 (t, 1H, bipy 5′-*H*), 5.54 (dd, 1H, bipy 3-*H*), 4.80 (dt, 1H, bipy 5-*H*), 4.17 (br m, 2H, fc-*H*), 4.12 (br m, 1H, bipy 4-*H*), 4.03 (br s, 4H, OCH_2CH_2), 4.02 (br s, 2H, fc-H) 3.56 (br m, 2H, fc-*H*) 3.12 (br m, 2H, fc-*H*), 3.12 (br m, 2H, CH_2Ar), 2.23 (s, 6H, C_6H_3-$(CH_3)_2$), 1.27 (br m, 4H, OCH_2CH_2), 0.94 and 0.91 (s, 9H each, $SiC(CH_3)_3$), 0.31, 0.21, −0.08, −0.11 (s, 3H each, $Si(CH_3)_2$). ^{13}C NMR (151 MHz, C_6D_6): *δ*, ppm: 159.3, 145.6, 145.1, 140.3, 137.61, 137.58, 135.7, 120.7, 120.2, 104.6, 104.3, 104.2, 99.1, 72.4, 67.8, 67.7, 67.01, 66.94, 65.7, 65.6, 65.4, 65.3, 49.9, 38.1, 35.0, 34.9, 29.4, 27.8, 27.7, 25.6, 25.1, 21.5, 20.9, 20.64, 20.58, −2.5, −2.6, −3.3, −3.4, −4.0.

Synthesis of 1^{Sc}−iqn. 1^{Sc}−THF (300 mg, 0.442 mmol) was dissolved in toluene (10 mL) and combined with a solution of 1 equiv of isoquinoline (57 mg, 0.442 mmol) in toluene (1 mL). The reaction mixture immediately turned orange and was stirred for 30 min at room temperature. The solvent was removed by vacuum and the resulting orange solid was washed with hexanes, extracted with toluene, filtered through Celite, and the volatiles were removed under vacuum. Yield: 203.3 mg, 62.5% as a solid obtained after toluene removal. ^{1}H NMR (500 MHz, C_6D_6): *δ*, ppm: 8.92 (s, 1H, iqn-C*H*), 8.22 (s, 1H, iqn-C*H*), 7.52 (d, 1H, iqn-C*H*), 7.23 (s, 2H, *o*-C_6H_3), 7.13−7.10 (m, 2H, iqn-C*H*), 7.05 (t, 1H, iqn-C*H*), 6.62 (s, 1H, *p*-C_6H_3), 4.22 (s, 2H fc-C*H*), 3.88 (s, 2H fc-C*H*), 3.56 (s, 4H, fc-C*H*), 3.01 (s, 2H, CH_2-Ar), 2.37 (s, 6H, C_6H_3-$(CH_3)_2$), 0.93 (s, 18H, $SiC(CH_3)_3$), −0.05 and −0.13 (s, 6H, $Si(CH_3)_2$). ^{13}C NMR (126 MHz, C_6D_6): *δ*, ppm: 153.9, 150.5, 140.3, 138.2, 136.7, 133.0, 128.9, 128.7, 126.7, 124.7, 121.6, 121.5, 106.0, 70.3, 68.5, 66.5, 55.1, 27.8, 21.9, 20.5, −2.4, −3.1. Anal. (%) for $C_{40}H_{56}FeN_3ScSi_2$ Calcd: C, 65.49; H, 7.67; N, 5.71; Found: C, 65.48; H, 7.59; N, 5.65.

Synthesis of 3^{Sc}−THF. 1^{Sc}−THF (200 mg, 0.295 mmol) was dissolved in C_6D_6 (1.5 mL) and combined with 1 equiv of isoquinoline (38 mg, 0.295 mmol) and a drop (2.5 mg) of THF. The reaction mixture immediately turned orange and was heated to 50 °C for 36 h. The solvent was removed under vacuum, hexanes was added to the resulting orange solid and filtered through Celite. The solution was concentrated and placed in a −35 °C freezer. The product was collected as crystals by decanting the mother liquor. Yield: 155 mg, 72.9%. ^{1}H NMR (300 MHz, C_6D_6): *δ*, ppm: 7.87 (d, 1H, iqn C3-*H*), 7.17 (m, 2H, iqn-C*H*), 7.01−6.93 (m, 2H, iqn-C*H*), 6.80 (s, 2H, *o*-C_6H_3), 6.89 (s, 1H, *p*-C_6H_3), 5.87 (d, 1H, iqn C4-*H*), 5.47 (t, 1H, iqn C1-*H*), 4.22 (s, 1H, fc-C*H*), 4.11 (s, 1H, fc-C*H*), 3.88−3.60 (m, 7H, fc-C*H* and OCH_2CH_2), 3.52, 3.37, and 3.28 (s, 1H, fc-C*H*), 3.12 (dd, 2H, iqn-CH_2), 2.18 (s, 6H, $C_6H_3CH_3$), 1.16 (br s, 4H, OCH_2CH_2), 1.05 and 1.02 (s, 9H, $SiC(CH_3)_3$), 0.27, 0.23, 0.16, and 0.12 (s, 3H, $SiCH_3$). Anal. (%) for $C_{44}H_{64}FeN_3OScSi_2$ Calcd: C, 65.41; H, 7.98; N, 5.20; Found: C, 64.58; H, 7.84; N, 5.43.

Synthesis of 3^{Y}−THF. 1^{Y}−THF (229.0 mg, 0.335 mmol) and isoquinoline (43.5 mg, 0.337 mmol) were combined in a capped 20-mL scintillation vial and stirred for 2 h in toluene at room temperature. The solvent was removed under vacuum, the resulting crude mixture was dissolved in hexanes and left at −35 °C overnight to precipitate **3^{Y}−THF**. The yield was 74.9% (206.8 mg, 0.251 mmol) of a yellow-orange powder.

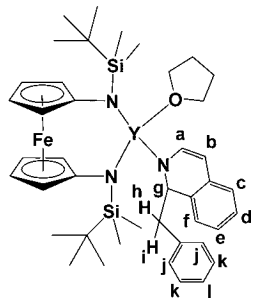

^{1}H NMR (500 MHz, C_6D_6): *δ*, ppm: 7.62 (d, 1H, *a*), 7.17 (br d, 4H, *c*, *d*, *e*, *f*), 7.08 (t, 2H, *k*), 7.01 (s, 2H, *j*), 6.96 (t, 1H, *l*), 5.88 (d, 1H, *b*), 5.20 (br s, 1H, *g*), 3.93 and 3.87 (br d, 4H, fc-*H*), 3.59 (br s, 4H, OCH_2CH_2), 3.32 (s, 4H, fc-*H*), 3.18 (br d, 1H, *h*), 2.92 (br d, 1H, *i*), 1.09 (br s, 4H, OCH_2CH_2), 1.02 (s, 18H, $SiC(CH_3)_3$), 0.17 and 0.12 (d, 12H, $Si(CH_3)_2$). ^{13}C NMR (126 MHz, C_6D_6): *δ*, ppm: 140.3, 140.2, 134.9, 130.4, 130.2, 128.1, 127.0, 126.8, 126.4, 125.5, 125.2, 122.8, 121.4, 108.2, 97.2, 70.6, 67.0, 61.9, 40.7, 27.7, 25.2, 20.5, −2.0, −2.2. Anal. (%) for $C_{42}H_{60}N_3OFeYSi_2$ Calcd: C, 61.23; H, 7.34; N, 5.10. Found: C, 61.61; H, 7.54; N, 5.27.

Synthesis of 3^{Lu}−THF. In a typical reaction, **1^{Lu}−THF** (177.9 mg, 0.220 mmol) was combined with 1 equiv of isoquinoline (28.4 mg, 0.220 mmol) in a vial and dissolved in about 5 mL of toluene. The solution became transparent red immediately. The reaction mixture was stirred for about 24 h at room temperature, after which it took on an orange hue. The solution was then filtered through Celite and dried under vacuum. The resulting orange solid was taken up in *n*-pentane. The *n*-pentane solution was then concentrated under vacuum and stored at −35 °C to afford yellow crystals. The mother liquor was removed, further concentrated under vacuum, and stored at −35 °C to afford a second crop of crystals. Total yield: 206.3 mg, 69.8%. Average yield for this reaction, over the course of 6 separate reactions, was 61.2%. ^{1}H NMR (500 MHz, C_6D_6): *δ*, ppm: 7.58 (d, 1H, iqn 3-*H*), 7.23, 7.21, 7.20, 7.14, 7.11, 7.10, 7.08, 7.07, 7.05, 7.02, 7.00 (m, 4H, iqn 5-*H*, 6-*H*, 7-*H* and 8-*H*), 6.87 (s, 2H, xylyl-C*H*), 6.67 (s, 1H, xylyl-C*H*), 5.98 (d, 1H, iqn 4-*H*), 5.20 (dd, 1H, iqn 1-*H*), 3.87 (br s, 4H, fc-*H*), 3.64 (br s, 4H, OCH_2CH_2), 3.42 (s, 2H, fc-*H*), 3.38 (dd, 1H, CH_2), 2.83 (dd, 1H, CH_2), 2.19 (s, 6H, xylyl-CH_3), 1.10 (br s, 4H, OCH_2CH_2), 1.04 (s, 18H, $SiC(CH_3)_3$), 0.18 and 0.12 (s, 6H each, $Si(CH_3)_2$). ^{13}C NMR (126 MHz, C_6D_6): *δ*, ppm: 141.3, 140.4, 137.1, 135.2, 131.6, 128.9, 127.5, 126.8, 125.9, 123.4, and 122.0 (aromatic *C* and Cp *C*-N), 108.9 (iqn 3-*C*), 98.8 (iqn 4-*C*), 71.3 (Cp *C*-H), 67.5 (OCH_2CH_2), 62.6 (Cp *C*-H), 40.2, 27.8, 25.3, 21.5, and 20.6 (methylene CH_2, isoquinoline 1-*C*, $SiC(CH_3)_3$, $Si(CH_3)_2$, and $C_6H_3(CH_3)_2$), −2.2 (OCH_2CH_2 and $SiC(CH_3)_3$). Anal. (%) for $C_{44}H_{64}N_3OSi_2FeLu$ Calcd: C, 56.34; H, 6.88; N, 4.48. Found: C, 56.41, H, 6.91, N, 4.57.

Synthesis of 3^{La}−THF. A toluene (8 mL) solution of **1^{La}−THF** (300 mg, 0.389 mmol) was combined with a toluene (1 mL) solution of isoquinoline (5 mg, 0.389 mmol) and the reaction mixture was stirred for 15 min at room temperature. The solvent was removed under vacuum, the resulting red solid was washed with hexanes, extracted in toluene, and filtered through Celite. The solution was concentrated, layered with *n*-pentane, and placed in a −35 °C freezer. The product was collected as crystals by decanting the mother liquor. Yield: 263 mg, 75%. ^{1}H NMR (500 MHz, C_6D_6): *δ*, ppm: 7.43 (d, 1H, iqn 3-*H*), 7.17 (m, 2H, iqn-C*H*), 6.88 (t, 1H, iqn-C*H*), 6.77 (s, 2H, *o*-C_6H_5), 6.72 (s, 1H, *p*-C_6H_5), 6.70 (d, 1H, iqn-C*H*), 5.79 (d, 1H, iqn 4-*H*), 5.21 (dd, 1H, iqn 1-*H*) 4.06 (s, 4H, fc-C*H*), 3.70, (br s, 8H, OCH_2CH_2), 3.51 (dd, 1H, CH_2Ph), 3.14 (s, 4H, fc-C*H*), 2.88 (dd, 1H, CH_2Ph), 2.20 (s, 6H, $C_6H_3(CH_3)_2$), 1.28 (br s, 8H, OCH_2CH_2), 1.04 (s, 18H, $SiC(CH_3)_3$), 0.33 and 0.27 (s, 6H, $Si(CH_3)_2$). ^{13}C NMR (126 MHz, C_6D_6): *δ*, ppm: 140.7, 140.6, 137.1, 136.6, 128.7, 127.6, 127.0, 126.6, 121.3, 120.8, 105.4, 93.6, 70.4, 66.4, 66.1, 66.0, 63.5, 40.6, 27.7, 25.3, 21.5, 20.5, −2.3, −2.4. Anal. (%) for $C_{44}H_{64}FeLaN_3OSi_2$: Calcd.: C, 58.59; H, 7.15; N, 4.66; Found: C, 58.81; H, 6.84; N, 4.42.

Synthesis of 3^{Y}−iqn^{Me}. 1^{Y}−THF (117.2 mg, 0.172 mmol) and 3 equiv of 3-methylisoquinoline (75.5 mg, 0.527 mmol) were combined in toluene in a capped 20-mL scintillation vial and stirred for 2 h, at room temperature. The solvent was removed under vacuum and the resulting crude mixture was dissolved in hexanes and left at −35 °C overnight, precipitating the desired product. The yield was 60.5% (94.6 mg, 0.104 mmol) of a red powder.

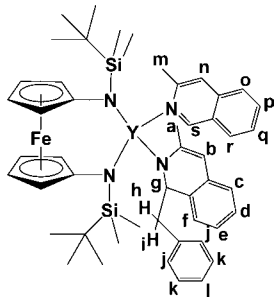

^{1}H NMR (500 MHz, C_6D_6): δ, ppm: 8.88 (s, 1H, *n*), 7.37 (d, 1H, *s*), 7.33, 7.26, 7.20, 7.10, 7.02, 6.98, 6.85 (m, 13H, *c, d, e, f, j, k, l, o, p, q, r*), 6.01 (s, 1H, *b*), 5.57 (dd, 1H, *g*), 4.25 (s, 1H, fc-C*H*), 4.11 (s, 1H, fc-C*H*), 3.85 (s, 1H, fc-C*H*), 3.75 (s, 1H, fc-C*H*), 3.68 (s, 1H, fc-C*H*), 3.63 (s, 1H, fc-C*H*), 3.60 (s, 1H, fc-C*H*), 3.54 (m, 1H, fc-C*H*), 2.81 (overlapped s, 2H, *h, i*), 2.72 (s, 3H, *m*), 2.71 (s, 3H, *a*), 0.94 (s, 9H, SiC(CH_3)$_3$), 0.92 (s, 9H, SiC(CH_3)$_3$), 0.11 (s, 3H, SiCH_3), −0.20 (s, 3H, SiCH_3), −0.41 (s, 3H, SiCH_3), −0.59 (s, 3H, SiCH_3).^{13}C NMR (126 MHz, C_6D_6): δ, ppm: 155.0, 149.5, 148.8, 140.1, 136.8, 135.8, 132.6, 130.9, 130.4, 129.1, 126.8, 126.4, 125.6, 125.3, 125.0, 122.7, 121.0, 120.9, 110.4, 109.4, 96.5, 69.7, 68.9, 68.6, 68.2, 66.4, 66.2, 65.7, 62.9, 61.0, 40.2, 34.5, 28.9, 27.7, 27.5, 26.8, 25.2, 20.6, 20.3, 11.2, −1.2, −2.8, −3.8, −4.1. Anal. (%) for $C_{49}H_{63}N_4FeYSi_2$ Calcd: C, 64.75; H, 6.99; N, 6.16. Found: C, 64.46; H, 7.02; N, 6.17.

Synthesis of 4^{Y}-(iqn)$_2$. 3^{Y}-THF (95.1 mg, 0.115 mmol) and 3 equiv of isoquinoline (44.8 mg, 0.347 mmol) were combined in a Schlenk tube and stirred in toluene for 6 h at 50 °C. The solvent was removed under vacuum and the resulting crude mixture was dissolved in hexanes and left at −35 °C overnight, precipitating the desired product. The yield was 72.0% (76.5 mg, 0.0831 mmol) of blood-red crystals and powder.

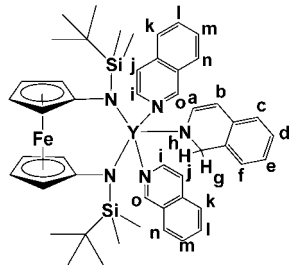

^{1}H NMR (500 MHz, C_6D_6): δ, ppm: 9.90 (s, 2H, *i*), 8.98 (s, 2H, *o*), 7.65 (d, 2H, *n*), 7.32, 7.23 through 7.18, 7.14 through 7.01, and 6.85 through 6.82 (m, 12H, *c, d, e, f, j, k, l, m*), 6.50 (d, 1H, *a*), 5.69 (d, 1H, *b*), 4.66 (s, 2H, *g, h*), 3.97 (s, 4H, fc-*H*), 3.20 (s, 4H, fc-*H*), 1.03 (s, 18H, SiC(CH_3)$_3$), 0.37 (s, 12H, Si(CH_3)$_2$). ^{13}C NMR (126 MHz, C_6D_6): δ, ppm: 154.7, 148.2, 142.5, 138.7, 136.6, 132.2, 128.7, 126.9, 126.7, 124.7, 122.0, 121.7, 120.3, 105.2, 95.4, 67.2, 66.7, 53.4, 28.1, 20.9, −1.8. Anal. (%) for $C_{49}H_{60}N_5FeYSi_2$ Calcd: C, 63.97; H, 6.57; N, 7.61. Found: C, 63.67; H, 6.28; N, 7.46.

Synthesis of 4^{Lu}−(iqn)$_2$. 3^{Lu}−THF (101.6 mg, 0.126 mmol) and 4 equiv of isoquinoline (65.1 mg, 0.502 mmol) were combined in a Schlenk tube with 5 mL of toluene. The solution immediately turned red. A stir bar was added and the solution was stirred at 50 °C for 30 h. The solution was next filtered through a fiber-glass filter and dried under vacuum, resulting in a red oil. The oil was triturated once with hexanes. The solid was then taken up in hexanes and concentrated under vacuum. The solution was stored at −35 °C, affording analytically pure red crystals. A second crop of crystals was also obtained after further concentration of the mother liquor. Total yield: 105.2 mg, 83.2%.

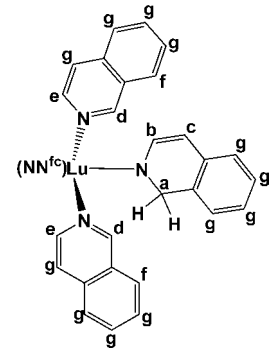

^{1}H NMR (300 MHz, C_6D_6): δ, ppm: 10.02 (s, 2H, *d*), 9.10 and 9.08 (d, 2H, *e*), 7.70 and 7.68 (d, 2H, *f*), 7.27 through 7.19, 7.14 through 7.01, and 6.86 through 6.81 (m, 11H, *g*), 6.45 and 6.42 (s, 2H, *b*), 5.71 and 5.68, (d, 1H, *c*), 4.56 (s, 2H, *a*), 3.93 (m, 4H, fc-*H*), 3.23 (br s, 4H, fc-*H*), 1.03 (s, 18H, SiC(CH_3)$_3$), 0.37 (s, 12H, Si(CH_3)$_2$). ^{13}C NMR (126 MHz, C_6D_6): δ, ppm: 155.1, 148.6, 142.9, 138.5, 136.7, 132.4, 128.8, 126.90, 126.87, 126.7, 124.8, 122.2, 121.7, 120.3, 104.4, 96.3, 67.4, 66.7, 53.7, 28.2, 21.2, −1.6. Anal. (%) for $C_{49}H_{60}N_5Si_2FeLu$ Calcd: C, 58.50; H, 6.01; N, 6.96. Found: C, 57.76, H, 5.51, N, 6.80.

Characterization of 5^{Ar}.

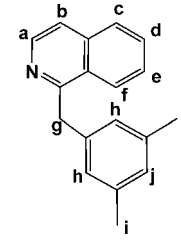

^{1}H NMR (300 MHz, C_6D_6): δ, ppm: 8.58 and 8.56 (d, 1H, *a*), 8.04 and 8.02 (d, 1H, *f*), 7.37 and 7.34 (d, 1H, *b*), 7.08 (m, 3H, *c*, *d* and *e*), 6.99 (s, 2H, *h*), 6.64, (s, 1H, *j*), 4.64 (s, 2H, *g*), 2.02 (s, 6H, *i*).

Synthesis of 6^{Lu}−(iqn)$_2$. 3^{Lu}−THF (133.0 mg, 0.142 mmol) and 2 equiv of 2-adamantanone (42.6 mg, 0.284 mmol) were combined in about 5 mL of toluene. The orange solution was stirred at room temperature for 3.5 h, after which it was dried under vacuum. The reaction was triturated once with hexanes, resulting in a foamy, orange oil, which weighed 175.9 mg. All attempts to crystallize the oil failed. ^{1}H NMR spectroscopy showed the product to be **6^{Lu}−iqn^{Ar}**, for which a molecular weight was calculated to be 1016.093 g/mol. Based upon this observation, 2 equiv of isoquinoline was added (44.7 mg, 0.346 mmol) and the reactants were dissolved in ∼3 mL of toluene. The solution was stirred for 2 h at room temperature, after which it was filtered through a fiberglass filter. The vial was washed with hexanes and the hexanes wash was also filtered through the fiberglass filter. The solvent was then removed under vacuum and the solid was taken up in *n*-pentane and stored at −35 °C, affording an orange powder. Total yield: 56.7 mg, 38.9%. ^{1}H NMR (500 MHz, C_6D_6): δ, ppm: 10.25 (br s, 2H, iqn 1-*H*), 9.24 (d, 2H, iqn 3-*H*), 7.86 and 7.84 (d, 2H, iqn 8-*H*) 7.30 and 7.29 (d, 2H, iqn 5-*H*), 7.26 and 7.24 (d, 2H, iqn 4-*H*), 7.20 (t, 2H, iqn 6-*H*) 7.11 (t, 2H, iqn 7-*H*) 4.55 (s, 1H, O−C*H*), 4.05 and 3.53 (s, 4H each, fc-*H*), 2.32 and 2.30 (d, 2H, ad-*H*), 2.02 (s, 2H, ad-*H*), 1.85 through 1.67 (m, 8H, ad-*H*), 1.41 and 1.39 (d, 2H, ad-*H*), 1.12 (s, 18H, SiC(CH_3)$_3$), 0.22 (s, 12H, Si(CH_3)$_2$). ^{13}C NMR (126 MHz, C_6D_6): δ, ppm: 154.6, 142.7, 136.5, 132.1, 126.8, 121.6, 105.3, 80.8, 67.1, 65.6, 38.6, 38.0, 37.7, 32.1, 28.7, 28.2, 28.1, 21.1, −2.0. Anal. (%) for $C_{50}H_{67}N_4OSi_2FeLu$ Calcd: C, 58.47; H, 6.58; N, 5.46. Found: C, 58.42, H, 6.45, N, 5.51.

Synthesis of 7^{Sc}−iqn^{Ar}. 3^{Sc}−THF (280 mg, 0.380 mmol) was combined with 1.05 equiv of benzophenone (72.8 mg, 0.400 mmol)

in toluene (10 mL) and stirred for 1 h at room temperature. The solvent was removed by vacuum and the resulting yellow solid was washed with hexanes (1 mL), extracted with toluene and filtered through Celite. Yield: 349 mg, 99%, as a solid obtained after the removal of the volatiles. ^{1}H NMR (500 MHz, C_6D_6): δ, ppm: 8.95 (s, 1H, iqn-C*H*), 8.21 (d, 1H, iqn-C*H*), 7.96 (d, 4H, *o*-C_6H_5), 7.48 (d, 1H, iqn-C*H*), 7.32 (t, 4H, *m*-C_6H_5), 7.10 (t, 2H, *p*-C_6H_5), 7.05 (t, 1H, iqn-C*H*), 6.85 (s, 2H, *o*-C_6H_5), 6.70 (s, 1H, *p*-C_6H_5), 4.26 (br s, 2H, fc-C*H*), 4.18 (s, 2H, CH_2-Ar), 3.82 (br s, 4H, fc-C*H*), 3.75 (br s, 2H, fc-C*H*), 2.09 (s, 6H, C_6H_3-(CH_3)$_2$), 0.93 (s, 18H, SiC(CH_3)$_3$), −0.18 (s, br, 12H, Si(CH_3)$_2$). The limited solubility of **7^{Sc}−iqn^{Ar}** prevented the collection of its ^{13}C NMR spectrum. Anal. (%) for $C_{53}H_{66}FeN_3OScSi_2$ Calcd: C, 69.34; H, 7.25; N, 4.58; Found: C, 69.10; H, 7.18; N, 4.58.

Synthesis of 7^{Y}−(iqn)$_2$. 3^{Y}−THF (51.0 mg, 0.0619 mmol) and benzophenone (11.6 mg, 0.0637 mmol) were combined in a capped 20-mL scintillation vial and stirred in toluene (3 mL) for 5 min at room temperature. A toluene solution (2 mL) with 2 equiv of isoquinoline (16.0 mg, 0.124 mmol) was added and the mixture was stirred for an additional 30 min at room temperature. The solvent was removed under vacuum and the resulting crude mixture was dissolved in hexanes and left at −35 °C overnight, precipitating the desired product. The yield was 62.3% (37.5 mg, 0.0386 mmol) of a pale-yellow powder.

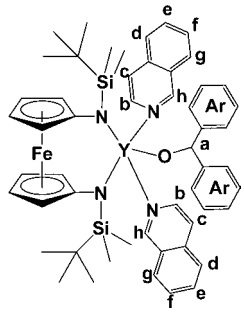

^{1}H NMR (500 MHz, C_6D_6): δ, ppm: 9.78 (s, 2H, *h*), 8.92 (s, 2H, *b*), 7.57, 7.22, 7.08, 6.95 (m, 16H, Ar, *d*, *e*, *f*, *g*), 6.84 (br s, 2H, *c*), 6.64 (s, 1H, *a*), 4.07 (s, 4H, fc-C*H*), 3.42 (s, 4H, fc-C*H*), 1.10 (s, 18H, SiC(CH_3)$_3$), 0.33 (s, 12H, Si(CH_3)$_2$). ^{13}C NMR (126 MHz, C_6D_6): δ, ppm: 154.2, 149.6, 141.7, 136.0, 131.3, 128.2, 126.9, 126.1, 125.4, 120.8, 105.7, 82.7, 66.3, 65.4, 27.5, 20.4, −2.4. Anal. (%) for $C_{53}H_{63}N_4OFeYSi_2$ Calcd: C, 65.42; H, 6.53; N, 5.76. Found: C, 65.36; H, 6.32; N, 5.74.

Synthesis of 7^{La}−(iqn)$_2$. A toluene (10 mL) solution of **3^{La}−THF** (263 mg, 0.291 mmol) was added to a toluene (1 mL) solution of 1.1 equiv of benzophenone (58 mg, 0.321 mmol) and the reaction mixture was stirred for 15 min at room temperature. The solvent was removed by vacuum and the resulting yellow solid was extracted with hexanes and filtered through Celite. After an unsuccessful attempt at crystallization as the THF solvate from hexanes, 2 equiv of isoquinoline (75 mg, 0.583 mmol) was added and the isoquinoline solvate was crystallized from hexanes. Yield: 168 mg, 56%. ^{1}H NMR (500 MHz, C_6D_6): δ, ppm: 9.53 (s, 2H, iqn-C*H*), 8.71, (d, 2H, iqn-C*H*), 7.70 (d, 4H, C_6H_5 or iqn-C*H*), 7.50 (d, 2H, C_6H_5 or iqn-C*H*), 7.22 (d, 2H, C_6H_5 or iqn-C*H*), 7.16 (t, 1H, C_6H_5 or iqn-C*H*), 7.09−7.05 (m, 8H, C_6H_5 or iqn-C*H*), 6.97 (t, 2H, C_6H_5 or iqn-C*H*), 6.71 (s, 1H, OC*H*), 4.13 (s, 4H, fc-C*H*), 3.40 (s, 4H, fc-C*H*), 1.03 (s, 18H, SiC(CH_3)$_3$), 0.39 (s, 12H, Si(CH_3)$_2$).^{13}C NMR (126 MHz, C_6D_6): δ, ppm: 153.8, 151.0, 141.8, 136.5, 131.7, 129.3, 128.6, 128.5, 127.5, 126.6, 126.1, 121.5, 107.4, 84.3, 65.7, 65.6, 27.6, 20.7, −2.5. Anal. (%) for $C_{53}H_{63}FeLaN_4OSi_2$ Calcd: C, 62.22; H, 6.21; N, 5.48; Found: C, 61.85; H, 6.25; N, 5.18.

Synthesis of 8^{Y}. 3^{Y}−THF (171.9 mg, 0.209 mmol) and azobenzene (40.0 mg, 0.220 mmol) were combined in a Schlenk tube and stirred in toluene for 24 h at 50 °C. The solvent was removed under vacuum and the resulting crude mixture was dissolved in *n*-pentane and left at −35 °C overnight, precipitating the desired product. The yield was 36.0% (73.9 mg, 0.0791 mmol) of a brown powder.

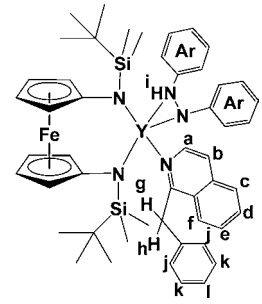

^{1}H NMR (300 MHz, C_6D_6, includes 1 equiv free toluene): δ, ppm: 9.11 (br s, 1H, *a*), 7.72 (d, 1H, *b*), 7.33 - 7.37, 7.21, 7.11, 7.07, 7.03, 6.93, 6.88, 6.85 (m, 24H, Ar, toluene, *c*, *d*, *e*, *f*, *j*, *k*, *l*), 6.22 (d, 1H, *i*), 5.04 (s, 2H, *g*, *h*), 4.15 (br s, 1H, fc-C*H*), 4.08 (br s, 1H, fc-C*H*), 3.97 (br s, 1H, fc-C*H*), 3.74 (br s, 1H, fc-C*H*), 3.66 (br s, 1H, fc-C*H*), 3.40 (br s, 1H, fc-C*H*), 3.16 (br s, 1H, fc-C*H*), 2.99 (br s, 1H, fc-C*H*), 2.11 (s, 3H, toluene), 0.88 (s, 18H, SiC(CH_3)$_3$), 0.13 (s, 6H, Si(CH_3)$_2$), −0.03 (s, 6H, Si(CH_3)$_2$). *Note*: Because of its solubility properties, **8^{Y}** could not be obtained pure enough for an elemental analysis study. As a result, **8^{Y}** was transformed into **8^{Y}−(iqn)$_2$**, which was fully characterized (see below).

Synthesis of 8^{Y}−(iqn)$_2$. 8^{Y} (73.9 mg, 0.0791 mmol) and 2 equiv of isoquinoline (20.5 mg, 0.159 mmol) were combined in a capped 20-mL scintillation vial and stirred for 2 h in toluene at room temperature. The solvent was removed under vacuum and the resulting crude mixture was dissolved in *n*-pentane and left at −35 °C overnight to precipitate the product. The yield was 55.2% (42.5 mg, 0.0437 mmol) of a beige powder.

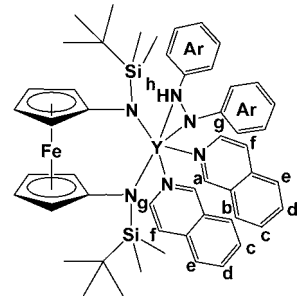

^{1}H NMR (500 MHz, C_6D_6): δ, ppm: 9.60 (br s, 2H, *g*), 8.88 (br s, 2H, *a*), 7.56, 7.21, 7.03, 6.89, 6.66, 6.58, 6.52, 6.21 (m, 20H, Ar, *b*, *c*, *d*, *e*, *f*), 6.27 (s, 1H, *h*), 4.12 (s, 2H, fc-C*H*), 3.87 (s, 2H, fc-C*H*), 3.60 (s, 2H, fc-C*H*), 2.90 (s, 2H, fc-C*H*), 1.12 (s, 18H, SiC(CH_3)$_3$), 0.52 (s, 6H, Si(CH_3)$_2$), 0.35 (s, 6H, Si(CH_3)$_2$). ^{13}C NMR (126 MHz, C_6D_6): δ, ppm: 154.7, 148.8, 135.8, 131.1, 128.8, 126.0, 121.0, 115.9, 114.9, 113.4, 105.4, 67.3, 67.0, 66.7, 65.4, 64.2, 61.3, 27.8, 26.2, 20.6, −1.5, −2.3. Anal. (%) for $C_{52}H_{63}N_6FeYSi_2$: Calcd.: C, 64.19; H, 6.53; N, 8.64. Found: C, 63.45; H, 6.15; N, 8.31.

Disproportionation Reaction of 3^{Y}−THF. 3^{Y}−THF (127.8 mg, 0.154 mmol) was dissolved in benzene in a Schlenk tube and heated without stirring for 3 d at 70 °C. The solution was then moved to a 20-mL scintillation vial, the solvent was removed, and a minimal amount of *n*-pentane was added to the crude mixture. The vial was left at −78 °C for one hour and the resulting liquid and solid were separated, dissolved in minimal *n*-pentane and left overnight at −35 °C, resulting in a orange powder (**4^{Y}−(THF)$_2$**) and a red compound, **9^{Y}**, that could not be fully separated before its decomposition. The yield for **4^{Y}−(THF)$_2$**was 94.4% (58.7 mg, 0.0728 mmol).

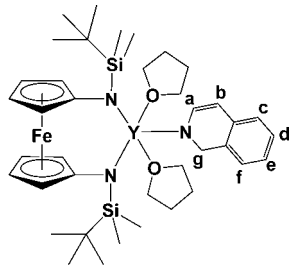

^{1}H NMR (300 MHz, C_6D_6): δ, ppm: 7.25 (overlap m, 2H, *a*, *c*), 7.10 (overlap m, 3H, *d*, *e*, *f*), 5.76 (d, 1H, *b*), 4.75 (s, 2H, *g*), 4.03 (s, 4H, fc-C*H*), 3.86 (s, 8H, O(CH_2CH_2)$_2$), 3.13 (s, 4H, fc-C*H*), 1.31 (s, 8H, OCH$_2$CH_2), 0.99 (s, 18H, SiC(CH_3)$_3$), 0.28 (s, 12H, Si(CH_3)$_2$). *Note*: Because of its solubility properties, the complex **4^{Y}−(THF)$_2$** could not be obtained pure enough for an elemental analysis study. As a result, **4^{Y}−(THF)$_2$** was transformed into **4^{Y}−(iqn)$_2$**, which was fully characterized (see below).

Reaction of 4^{Y}-(THF)$_2$ with Isoquinoline to Form 4^{Y}−(iqn)$_2$. 23.4 mg (0.0291 mmol) of **4^{Y}−(THF)$_2$**and 2.1 equiv of isoquinoline (7.9 mg, 0.0612 mmol) were dissolved and combined in C_6D_6 in an NMR tube fitted with a Teflon stopper. The solution was monitored and the reaction was determined to be complete after 2 h. The solution was moved to a 20-mL scintillation vial and the solvent was removed. A minimal amount of hexanes was added to the crude reaction mixture and the resulting solution was kept overnight at −35 °C, yielding a blood-red powder. Yield: 36.6% (9.8 mg, 0.0107 mmol).

Disproportionation Reaction of 3^{La}−THF. 3^{La}−THF was prepared in situ by the reaction of **1^{La}−THF** (200 mg, 0.269 mmol) with 1 equiv of isoquinoline (34.7 mg, 0.269 mmol) in C_6D_6 (1.5 mL). This reaction mixture was heated to 50 °C for 96 h. The solvent was removed by vacuum; a red product, identified as **9^{La}**, was extracted with hexanes, and filtered through Celite. An orange product identified as **4^{La}−(THF)$_2$** was extracted with toluene and filtered through Celite. Yield: 45 mg of **9^{La}**, 38.4%, as crystals from *n*-pentane, and 30 mg of **4^{La}−(THF)$_2$**, 26.1%, as crystals from toluene: *n*-pentane. Crystals of **9^{La}** suitable for X-ray diffraction were obtained from the analogous reaction of the 3,5-dimethylbenzyl complex from toluene: *n*-pentane. **4^{La}−(THF)$_2$**was not characterized because it could not be obtained in sufficient amount, as a consequence of its solubility properties and its decomposition to intractable products. **9^{La}**:^{1}H NMR (500 MHz, C_6D_6): δ, ppm: 8.13 (d, 1H, iqn-C*H*), 7.94 (s, 1H, iqn-C*H*), 7.89 (s, 2H, iqn-C*H*), 7.31−7.20 (m, 4H, C_6H_5 or iqn-C*H*), 6.77 (t, 1H, C_6H_5 or iqn-C*H*), 6.43 (s, 1H, C_6H_5 or iqn-C*H*), 6.02 (s, 1H, La−C*H*), 4.01 (s, 4H, fc-C*H*), 3.57 (s, 4H, OCH_2CH$_2$), 3.09 (s, 4H fc-C*H*), 1.28 (s, 4H, OCH$_2$CH_2), 0.96 (s, 18H, SiC(CH_3)$_3$), 0.01 (s, 12H, Si(CH_3)$_2$). ^{13}C NMR (126 MHz, C_6D_6): δ, ppm: 154.2, 143.4, 140.6, 137.0, 132.3, 130.1, 126.5, 125.9, 125.1, 121.9, 121.2, 106.9, 79.8, 70.0, 66.5, 27.6, 25.4, 20.5, −2.8. Anal. (%) for $C_{42}H_{58}FeN_3LaOSi_2$ Calcd: C, 57.86; H, 6.70; N, 4.82; Found: C, 57.92; H, 6.69; N, 4.86.

Disproportionation Reaction of Deuterium-Labeled 3^{La}−THF. 1^{La}−THF (100 mg, 0.134 mmol) was combined with 1 equiv of isoquinoline-*d* (17.5 mg, 0.134 mmol) in C_6H_6 (1.5 mL). A portion of the reaction mixture (0.5 mL) was separated and the solvent removed under vacuum. The resulting red-orange solid was dissolved in C_6D_6 (0.75 mL) and placed in a J-Young NMR tube. The remaining C_6H_6 solution was also placed in a J-Young tube. The two samples were heated to 50 °C and monitored by ^{1}H and ^{2}H NMR spectroscopy, respectively. After 48 h a peak at 2.08 ppm was observed by ^{2}H NMR spectroscopy that was attributed to deuterium incorporation in the liberated toluene.

X-Ray Crystal Structures. X-ray quality crystals were obtained from various concentrated solutions placed in a −35 °C freezer in the glovebox. Inside the glovebox, the crystals were coated with oil (STP Oil Treatment) on a microscope slide, which was brought outside the glovebox. The X-ray data collections were carried out on a Bruker AXS single crystal X-ray diffractometer using Mo Kα radiation and a SMART APEX CCD detector. The data was reduced by SAINTPLUS and an empirical absorption correction was applied using the package SADABS. The structures were solved and refined using SHELXTL (Bruker 1998, SMART, SAINT, XPREP AND SHELXTL, Bruker AXS Inc., Madison, Wisconsin, USA).[117] All atoms were refined anisotropically and hydrogen atoms were placed in calculated positions unless specified otherwise. Tables with atomic coordinates and equivalent isotropic displacement parameters, with all the bond lengths and angles, and with anisotropic displacement parameters are listed in the cifs.

X-Ray Crystal Structure of 1′^{La}−THF. X-ray quality crystals were obtained from a concentrated toluene: *n*-pentane solution placed in a −35 °C freezer in the glovebox. A total of 33077 reflections ($-25 \le h \le 25$, $-23 \le k \le 22$, $-15 \le l \le 14$) were collected at $T = 100(2)$ K with $2\theta_{max} = 56.54°$, of which 9094 were unique ($R_{int} = 0.0613$). The residual peak and hole electron density were 0.67 and −0.51 eA^{-3}. The least-squares refinement converged normally with residuals of $R_1 = 0.0364$ and GOF = 1.006. Crystal and refinement data for **1′^{La}−THF**: formula $C_{35}H_{57}N_2Si_2FeOLa$, space group *P*na2$_1$, $a = 19.018(3)$, $b = 17.284(3)$, $c = 11.281(2)$, $\alpha = \beta = \gamma = 90°$, $V = 3708.1(11)$ Å^3, $Z = 4$, $\mu = 1.620$ mm^{-1}, $F(000) = 1600$, $R_1 = 0.0437$ and $wR_2 = 0.0657$ (based on all 9094 data, $I > 2\sigma(I)$).

X-Ray Crystal Structure of 2^{Sc}. X-ray quality crystals were obtained from a concentrated toluene: *n*-pentane solution placed in a −35 °C freezer in the glovebox. A total of 22432 reflections ($-14 \le h \le 15$, $-19 \le k \le 19$, $-21 \le l \le 21$) were collected at $T = 100(2)$ K with $2\theta_{max} = 56.52°$, of which 12025 were unique ($R_{int} = 0.0463$). The residual peak and hole electron density were 1.85 and −0.69 eA^{-3}. The least-squares refinement converged normally with residuals of $R_1 = 0.0581$ and GOF = 1.024. One molecule of toluene solvent was found in the unit cell. Some of the methyl groups were thermally disordered; the disorder was not extensive and was not modeled. Crystal and refinement data for **2^{Sc}**: formula $C_{52}H_{73}N_4Si_2FeScO$, space group $P\bar{1}$, $a = 11.4536(19)$, $b = 14.490(2)$, $c = 16.233(3)$, $\alpha = 97.870(2)°$, $\beta = 98.337(2)°$, $\gamma = 106.382(2)°$, $V = 2512.0(7)$ Å^3, $Z = 2$, $\mu = 0.511$ mm^{-1}, $F(000) = 992$, $R_1 = 0.0926$ and $wR_2 = 0.1530$ (based on all 12025 data, $I > 2\sigma(I)$).

X-Ray Crystal Structure of 3^{Y}−iqn^{Me}. X-ray quality crystals were obtained from a concentrated hexanes solution placed in a −35 °C freezer in the glovebox. A total of 41770 reflections ($-18 \le h \le 19$, $-21 \le k \le 22$, $-26 \le l \le 26$) were collected at $T = 125(2)$ K with $2\theta_{max} = 56.59°$, of which 11372 were unique ($R_{int} = 0.0749$). The residual peak and hole electron density were 0.53 and −0.43 eA^{-3}. The least-squares refinement converged normally with residuals of $R_1 = 0.0469$ and GOF = 0.961. Crystal and refinement data for **3^{Y}−iqn^{Me}**: formula $C_{49}H_{63}N_4Si_2FeY$, space group *P*na2$_1$, $a = 14.3694(13)$, $b = 16.5282(14)$, $c = 19.6525(17)$, $\alpha = \beta = \gamma = 90°$, $V = 4667.5(7)$ Å^3, $Z = 4$, $\mu = 1.636$ mm^{-1}, $F(000) = 1912$, $R_1 = 0.0708$ and $wR_2 = 0.0979$ (based on all 11372 data, $I > 2\sigma(I)$).

X-Ray Crystal Structure of 4^{Lu}−(iqn)$_2$. X-ray quality crystals were obtained from a concentrated hexanes solution layered with *n*-pentane and placed in a −35 °C freezer in the glovebox. A total of 22108 reflections ($-18 \le h \le 18$, $-18 \le k \le 18$, $-19 \le l \le 19$) were collected at $T = 100(2)$ K with $2\theta_{max} = 56.70°$, of which 12008 were unique ($R_{int} = 0.0282$). The residual peak and hole electron density were 1.18 and −0.80 eA^{-3}. The least-squares refinement converged normally with residuals of $R_1 = 0.0316$ and GOF = 1.004. Some of the methyl groups were thermally disordered; the disorder was not extensive and was not modeled. Crystal and refinement data for **4^{Lu}-(iqn)$_2$**: formula $C_{52}H_{64}N_5Si_2FeLu$, space group $P\bar{1}$, $a = 13.908(2)$, $b = 13.942(5)$, $c = 14.914(3)$, $\alpha = 95.659(2)$, $\beta = 116.825(2)$, $\gamma = 98.466(2)°$, $V =$

(117) Sheldrick, G. *Acta Cryst. A* **2008**, *64*, 112–122.

2507.6(10) Å^3, $Z = 2$, $\mu = 2.333$ mm^{-1}, $F(000) = 1072$, $R_1 = 0.0408$ and $wR_2 = 0.0694$ (based on all 12008 data, $I > 2\sigma(I)$).

X-Ray Crystal Structure of $4'^{Y}$−1,5-(py)$_2$. X-ray quality crystals were obtained from a concentrated *n*-pentane solution and placed in a −35 °C freezer in the glovebox. A total of 23359 reflections ($-36 \le h \le 36$, $-17 \le k \le 17$, $-19 \le l \le 19$) were collected at $T = 100(2)$ K with $2\theta_{max} = 56.53°$, of which 6404 were unique ($R_{int} = 0.0563$). The residual peak and hole electron density were 1.05 and −0.52 eA^{-3}. The unit cell contains one molecule of *n*-pentane or hexane, which was very disordered. A good model could not be obtained for the solvent because of its disorder and of the fact that some of the atoms sit in special positions. After successive failed attempts to find a proper solvent model, no carbon atoms were fitted to the electron density corresponding to the solvent molecule. Some of the methyl groups were thermally disordered; the disorder was not extensive and was not modeled. The least-squares refinement converged normally with residuals of $R_1 = 0.0627$ and GOF = 1.196. Crystal and refinement data for **$4'^{Y}$-1,5-(py)$_2$**: formula $C_{37}H_{54}N_5Si_2FeY$, space group *C*2/c, $a = 27.282(3)$, $b = 13.0297(15)$, $c = 14.8077(17)$, $\beta = 99.407(1)°$, $V = 5192.9(10)$ Å^3, $Z = 4$, $\mu = 1.461$ mm^{-1}, $F(000) = 1616$, $R_1 = 0.0927$ and $wR_2 = 0.2318$ (based on all 6404 data, $I > 2\sigma(I)$).

X-Ray Crystal Structure of 6^{Lu}−(iqn)$_2$. X-ray quality crystals were obtained from a concentrated hexanes solution placed in a −35 °C freezer in the glovebox. A total of 43149 reflections ($-32 \le h \le 32$, $-15 \le k \le 15$, $-22 \le l \le 22$) were collected at $T = 101(2)$ K with $2\theta_{max} = 56.63°$, of which 11870 were unique ($R_{int} = 0.0964$). The residual peak and hole electron density were 0.72 and −0.88 eA^{-3}. The least-squares refinement converged normally with residuals of $R_1 = 0.0454$ and GOF = 0.978. One of the *t*-butyl groups was disordered over two sites (40 and 60% occupancy). One of the disordered counterparts was only refined isotropically. Crystal and refinement data for **6^{Lu}−(iqn)$_2$**: formula $C_{50}H_{67}N_4Si_2FeOLu$, space group *P*na2$_1$, $a = 24.396(10)$, $b = 11.830(5)$, $c = 16.723(7)$, $\alpha = \beta = \gamma = 90°$, $V = 4826(4)$ Å^3, $Z = 4$, $\mu = 2.423$ mm^{-1}, $F(000) = 2112$, $R_1 = 0.0668$ and $wR_2 = 0.0789$ (based on all 11870 data, $I > 2\sigma(I)$).

X-Ray Crystal Structure of 8^{Y}. X-ray quality crystals were obtained from a concentrated toluene: Et_2O solution placed in a −35 °C freezer in the glovebox. A total of 41841 reflections ($-49 \le h \le 49$, $-58 \le k \le 59$, $-14 \le l \le 14$) were collected at $T = 101(2)$ K with $2\theta_{max} = 52.80°$, of which 10820 were unique ($R_{int} = 0.1027$). The residual peak and hole electron density were 1.94 and −0.61 eA^{-3}. The least-squares refinement converged normally with residuals of $R_1 = 0.0579$ and GOF = 1.001. Crystal and refinement data for **8^{Y}**·C_7H_8: formula $C_{57}H_{70}N_5Si_2FeY$, space group *F*dd2, $a = 39.536(4)$, $b = 47.303(4)$, $c = 11.3457(10)$, $\alpha = \beta = \gamma = 90°$, $V = 21218(3)$ Å^3, $Z = 16$, $\mu = 1.448$ mm^{-1}, $F(000) = 8640$, $R_1 = 0.0807$ and $wR_2 = 0.1336$ (based on all 10820 data, $I > 2\sigma(I)$).

X-Ray Crystal Structure of 4^{Y}−(THF)$_2$. X-ray quality crystals were obtained from a concentrated *n*-hexane solution placed in a −35 °C freezer in the glovebox. A total of 36317 reflections ($-13 \le h \le 13$, $-38 \le k \le 38$, $-18 \le l \le 18$) were collected at $T = 109(2)$ K with $2\theta_{max} = 56.50°$, of which 9909 were unique ($R_{int} = 0.0978$). The residual peak and hole electron density were 0.56 and −0.42 eA^{-3}. The least-squares refinement converged normally with residuals of $R_1 = 0.0521$ and GOF = 0.983. Two methyl groups were disordered over two sites (50% occupancy each). Crystal and refinement data for **4^{Y}−(THF)$_2$**: formula $C_{39}H_{62}N_3Si_2FeO_2Lu$, space group $P2_1/c$, $a = 10.065(3)$, $b = 29.126(7)$, $c = 14.029(4)$, $\beta = 100.204(3)°$, $V = 4047.4(18)$ Å^3, $Z = 4$, $\mu = 1.880$ mm^{-1}, $F(000) = 1704$, $R_1 = 0.1070$ and $wR_2 = 0.1082$ (based on all 9909 data, $I > 2\sigma(I)$).

X-Ray Crystal Structure of 9^{La}. X-ray quality crystals were obtained from a concentrated toluene: *n*-pentane solution placed in a −35 °C freezer in the glovebox. A total of 30464 reflections ($-54 \le h \le 53$, $-11 \le k \le 11$, $-23 \le l \le 24$) were collected at $T = 100(2)$ K with $2\theta_{max} = 50.07°$, of which 7562 were unique ($R_{int} = 0.1188$). The residual peak and hole electron density were 0.50 and −0.52 eA^{-3}. The least-squares refinement converged normally with residuals of $R_1 = 0.0497$ and GOF = 0.991. Crystal and refinement data for **9^{La}**: formula $C_{44}H_{62}N_3Si_2FeOLa$, space group *C*2/c, $a = 45.634(13)$, $b = 9.376(3)$, $c = 20.379(6)$, $\beta = 99.243(3)°$, $V = 8606(4)$ Å^3, $Z = 8$, $\mu = 1.408$ mm^{-1}, $F(000) = 3728$, $R_1 = 0.0982$ and $wR_2 = 0.0907$ (based on all 7562 data, $I > 2\sigma(I)$).

Computational Details. Density functional theory (DFT) calculations were performed using the B3LYP functional (as implemented in Jaguar 7.6, release 110). Main group atoms were described using the 6-311++G** basis set,[118] while the LACV3P++**(2f), a small core effective potentials (angular momentum projected pseudopotentials) including a double-ζ f-type shell, was used for all metals.[119−122] Structures were optimized in the gas phase (starting with geometries obtained from the X-ray crystal structures where available) using the LACVP** and 6-31G** basis sets.[119,123] For stationary points and transition structures, the analytic Hessian was calculated to obtain vibrational frequencies, which in turn were used to obtain zero-point and vibrational thermodynamic corrections (ZPE, H(T), and S). Solvent corrections were based on single point self-consistent Poisson−Boltzmann continuum solvation calculations for benzene ($\varepsilon = 2.284$ and $R_0 = 2.60$ Å), toluene ($\varepsilon = 2.379$ and $R_0 = 2.76$ Å) or tetrahydrofuran ($\varepsilon = 7.6$ and $R_0 = 2.52$ Å) as noted using the PBF module in Jaguar.[124,125]

Acknowledgment. P.L.D. thanks Prof. James Mayer, University of Washington, Seattle, for a useful suggestion, Dr. Saeed Khan, UCLA, for help with some cyrstallography details, and Dr. Robert Taylor, UCLA, for help with NMR spectroscopy experiments. C.T.C. and K.R.O. thank Mr. Samuel I. Roth, Harvard-Westlake School, for the synthesis of La(CH$_2$C$_6$H$_5$)$_3$(THF)$_3$ and **1^{La}−THF**. The experimental work was supported by the UCLA, Sloan Foundation, and NSF (Grant CHE-0847735). The MSC computational facilities were funded by grants from ARO−DURIP and ONR-DURIP. E.T. gratefully acknowledges support from UC MEXUS-CONACyT for a postdoctoral fellowship. D.B., E.T., and W.A.G. were supported partially by the Center for Catalytic Hydrocarbon Functionalization, an Energy Frontier Research Center funded by the DOE (DE-SC0001298).

Supporting Information Available: Experimental details for compound characterizations, structural representations indicating a full atom-labeling scheme, DFT calculation details, and full crystallographic descriptions. This material is available free of charge via the Internet at http://pubs.acs.org.

JA908489P

(118) Krishnan, R.; Binkley, J. S.; Seeger, R.; Pople, J. A. *J. Chem. Phys.* **1980**, *72*, 650–654.
(119) Hay, P. J.; Wadt, W. R. *J. Chem. Phys.* **1985**, *82*, 299–310.
(120) Melius, C. F.; Goddard, W. A. *Phys. Rev. A* **1974**, *10*, 1541.
(121) Melius, C. F.; Olafson, B. D.; Goddard, W. A. *Chem. Phys. Lett.* **1974**, *28*, 457–462.
(122) Martin, J. M. L.; Sundermann, A. *J. Chem. Phys.* **2001**, *114*, 3408–3420.
(123) Ditchfield, R.; Hehre, W. J.; Pople, J. A. *J. Chem. Phys.* **1971**, *54*, 724–728.
(124) Tannor, D. J.; Marten, B.; Murphy, R.; Friesner, R. A.; Sitkoff, D.; Nicholls, A.; Honig, B.; Ringnalda, M.; Goddard, W. A. *J. Am. Chem. Soc.* **1994**, *116*, 11875–11882.
(125) Marten, B.; Kim, K.; Cortis, C.; Friesner, R. A.; Murphy, R. B.; Ringnalda, M. N.; Sitkoff, D.; Honig, B. *J. Phys. Chem.* **1996**, *100*, 11775–11788.